Atrial Fibrillation: Modeling Overview

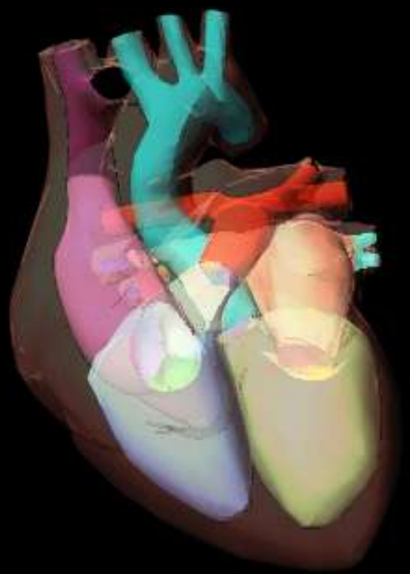

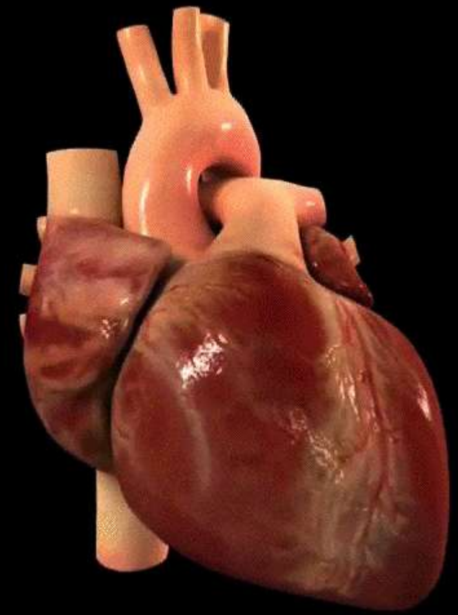

Flavio H. Fenton
Cornell University

Normal sinus rhythm

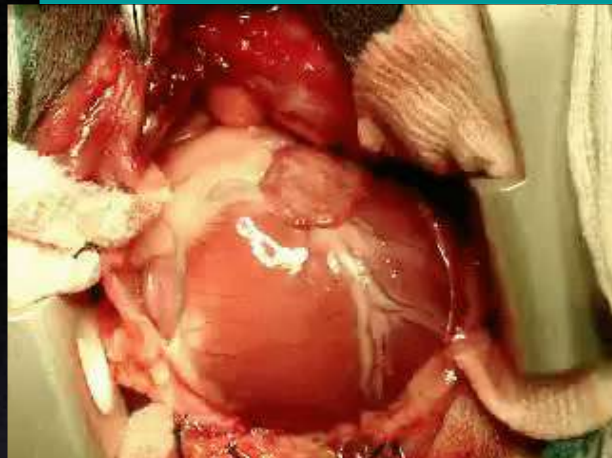

Atrial fibrillation

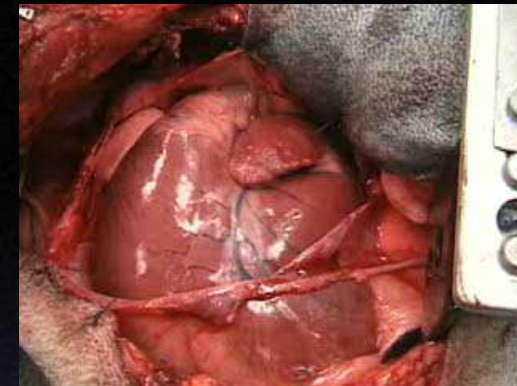

Ventricular tachycardia

Ventricular fibrillation

What Underlies Arrhythmias?

To understand how arrhythmias form, we must go beyond the mechanical function of the heart to the electrical.
Arrhythmias develop from disruptions in the normal electrical activation of the heart.
How does electricity play a role in the heart, and how do such disruptions of normal electrical activity occur?

Cellular Electrophysiology

- Cardiac cells are about 100-150 μm in length, 10-20 μm in diameter.
- The cell membrane: lipid bi-layer 10 nm thick, impermeable to ions except through specialized proteins (ion channels).
- Ion concentration gradient and voltage drop across membrane.
- Movement of ions across the membrane produces an action potential.
- Active transport through pumps and exchangers in the membrane restores original concentrations.

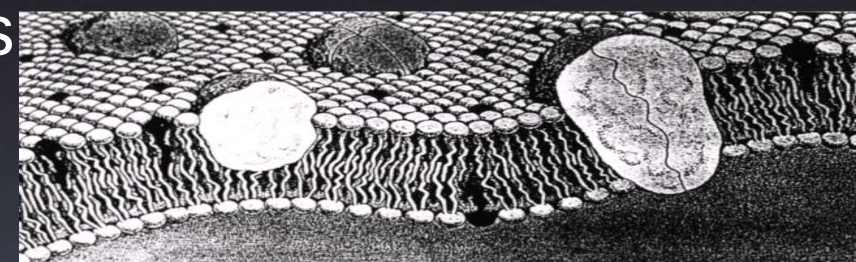

Cellular Electrophysiology

If the applet does not start go to:
http://thevirtualheart.org/java/cardiac/apcardiac.html

Ca^{2+}, Na^{+}, K^{+}

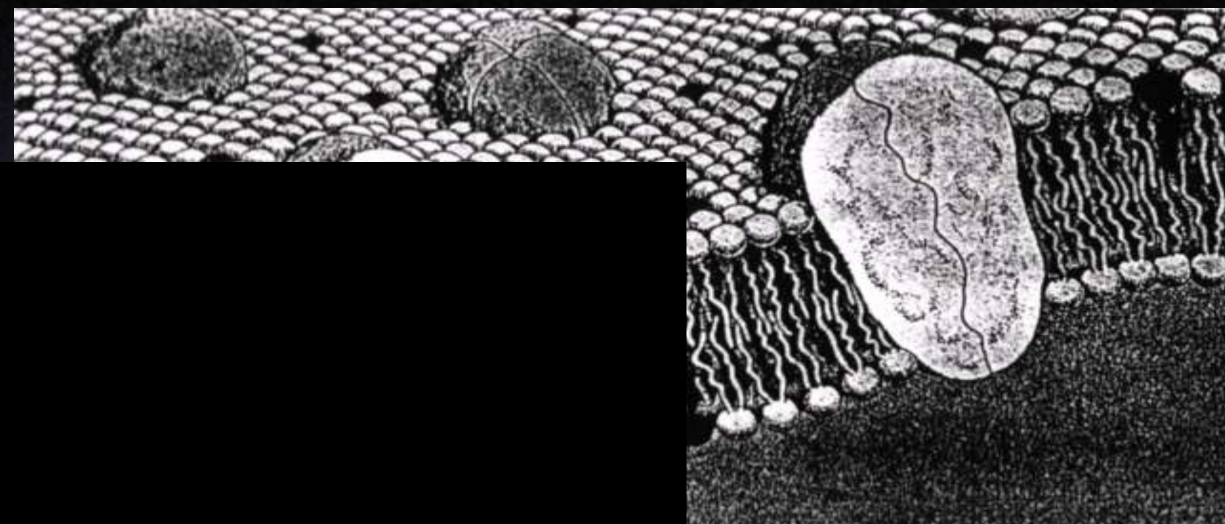

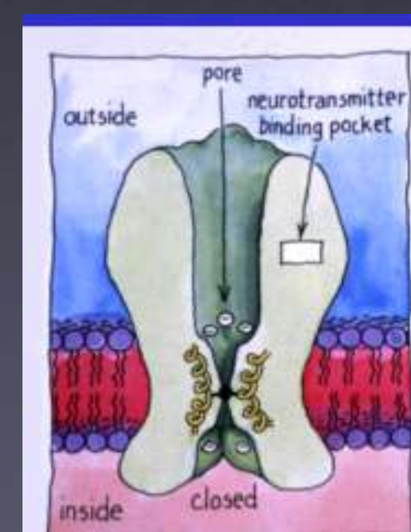

Electrical-Contraction Coupling

- Cellular action potential triggers contraction through calcium processes.
- Increased calcium current stimulates release of intracellular store.
- Transiently increased calcium binds to contraction proteins.

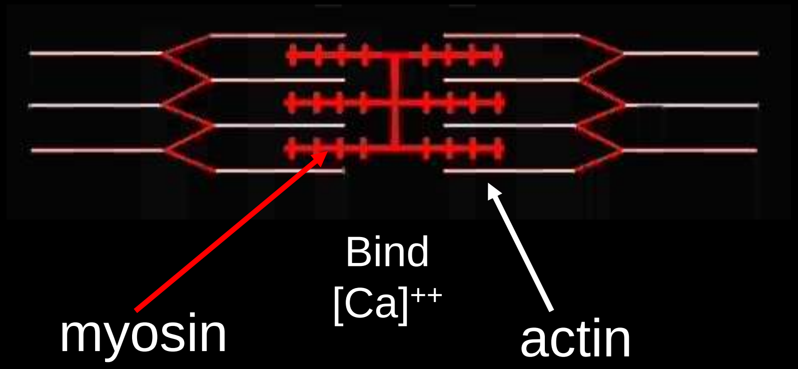

Modeling Cell Electrophysiology

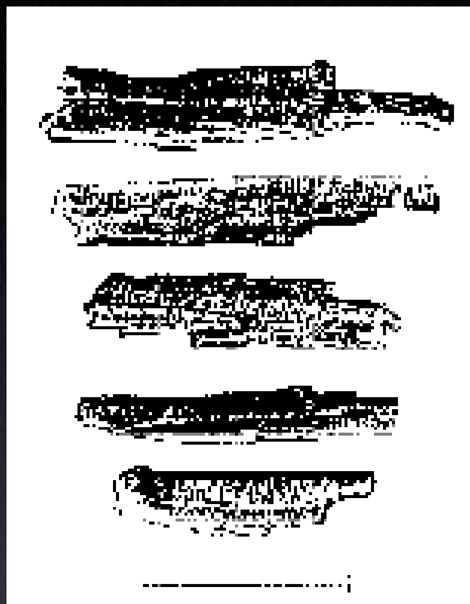

100 microns

Cell membrane thickness: 10 nanometers

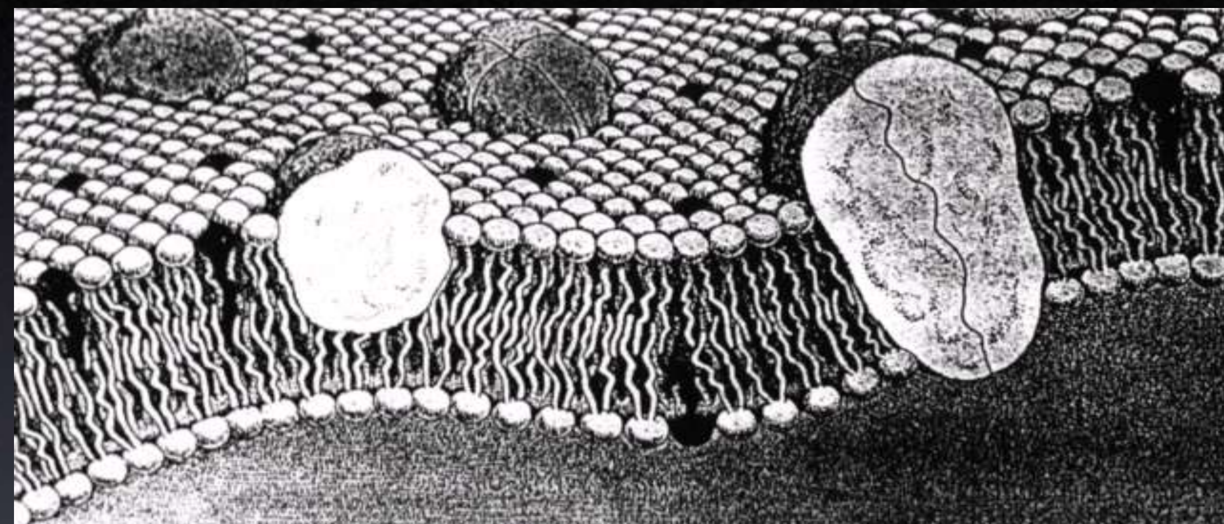

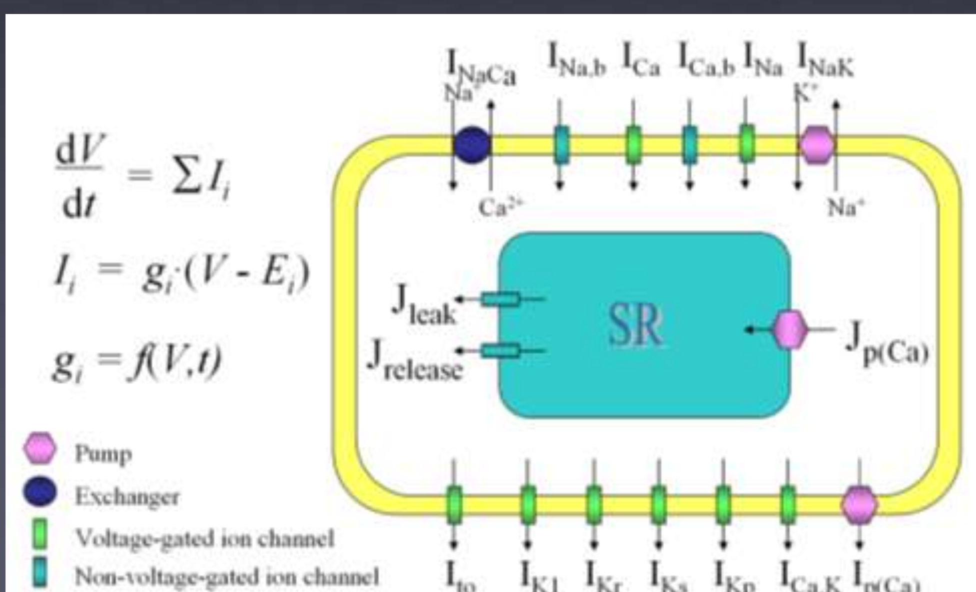

The cell membrane is a lipid bilayer impermeable to ions except through specialized structures.

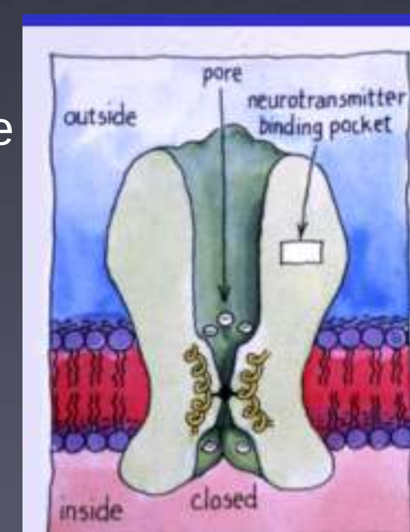

TABLE 4 Initial conditions (pacing protocol)

State	Symbol	0.25 Hz
Membrane potential, mV	V	$-9.121\,E^{+01}$
Intracellular sodium, mM	$[Na^+]_i$	$8.006\,E^{+00}$
Intracellular potassium, mM	$[K^+]_i$	$1.274\,E^{+02}$
Intracellular calcium, mM	$[Ca^{2+}]_i$	$4.414\,E^{-05}$
NSR calcium, mM	$[Ca^{2+}]_{NSR}$	$1.741\,E^{-01}$
SS calcium, mM	$[Ca^{2+}]_{SS}$	$4.803\,E^{-05}$
JSR calcium, mM	$[Ca^{2+}]_{JSR}$	$1.741\,E^{-01}$
RyR state C_1	P_{C1}	$9.366\,E^{-01}$
RyR state O_1	P_{O1}	$7.516\,E^{-05}$
RyR state C_2	P_{C2}	$6.337\,E^{-02}$
RyR state O_2	P_{O2}	$1.749\,E^{-11}$
L-type state C_0	C_{0L}	$9.861\,E^{-01}$
L-type state C_1	C_{1L}	$1.251\,E^{-02}$
L-type state C_2	C_{2L}	$5.955\,E^{-05}$
L-type state C_3	C_{3L}	$1.260\,E^{-07}$
L-type state C_4	C_{4L}	$9.990\,E^{-11}$
L-type state O	O_L	$7.493\,E^{-12}$
L-type state C_{ca0}	C_{Ca0L}	$1.210\,E^{-03}$
L-type state C_{ca1}	C_{Ca1L}	$6.140\,E^{-05}$
L-type state C_{ca2}	C_{Ca2L}	$1.169\,E^{-06}$
L-type state C_{ca3}	C_{Ca3L}	$9.889\,E^{-09}$
L-type state C_{ca4}	C_{Ca4L}	$3.137\,E^{-11}$
L-type inactivation variable	y	$9.997\,E^{-01}$
High affinity troponin bound fraction	$HTRPN_{Ca}$	$9.359\,E^{-01}$
Low affinity troponin bound fraction	$LTRPN_{Ca}$	$4.233\,E^{-02}$
Kv4.3 state C_1	C_{1Kvf}	$9.527\,E^{-01}$
Kv4.3 state C_2	C_{2Kvf}	$2.563\,E^{-02}$
Kv4.3 state C_3	C_{3Kvf}	$2.586\,E^{-04}$
Kv4.3 state C_4	C_{4Kvf}	$1.159\,E^{-06}$
Kv4.3 state O	O_{Kvf}	$1.949\,E^{-09}$
Kv4.3 state CI_1	CI_{1Kvf}	$1.514\,E^{-02}$
Kv4.3 state CI_2	CI_{2Kvf}	$5.225\,E^{-03}$
Kv4.3 state CI_3	CI_{3Kvf}	$9.131\,E^{-04}$
Kv4.3 state CI_4	CI_{4Kvf}	$8.401\,E^{-05}$
Kv4.3 state I	OI_{1Kvf}	$2.323\,E^{-06}$
Kv1.4 state C_1	C_{1Kvs}	$7.630\,E^{-01}$
Kv1.4 state C_2	C_{2Kvs}	$2.108\,E^{-01}$
Kv1.4 state C_3	C_{3Kvs}	$2.184\,E^{-02}$
Kv1.4 state C_4	C_{4Kvs}	$1.006\,E^{-03}$
Kv1.4 state O	O_{Kvs}	$1.737\,E^{-05}$
Kv1.4 state CI_1	CI_{1Kvs}	$6.505\,E^{-04}$
Kv1.4 state CI_2	CI_{2Kvs}	$9.517\,E^{-05}$
Kv1.4 state CI_3	CI_{3Kvs}	$3.820\,E^{-04}$
Kv1.4 state CI_4	CI_{4Kvs}	$5.143\,E^{-04}$
Kv1.4 state I	OI_{1Kvs}	$1.719\,E^{-03}$
I_{Kr} state C_1	C_{1Kr}	$9.967\,E^{-01}$
I_{Kr} state C_2	C_{2Kr}	$4.163\,E^{-04}$
I_{Kr} state C_3	C_{3Kr}	$7.321\,E^{-05}$
I_{Kr} state O	O_{Kr}	$8.847\,E^{-06}$
I_{Kr} state I	I_{Kr}	$1.387\,E^{-06}$
I_{Ks} state C_0	C_{0Ks}	$9.646\,E^{-01}$
I_{Ks} state C_1	C_{1Ks}	$3.543\,E^{-02}$
I_{Ks} state O_1	O_{1Ks}	$2.294\,E^{-07}$
I_{Ks} state O_2	O_{2Ks}	$4.680\,E^{-11}$
I_{Na} state C_0	C_{0Na}	$1.474\,E^{-01}$
I_{Na} state C_1	C_{1Na}	$4.051\,E^{-02}$
I_{Na} state C_2	C_{2Na}	$4.175\,E^{-03}$
I_{Na} state C_3	C_{3Na}	$1.913\,E^{-04}$
I_{Na} state C_4	C_{4Na}	$3.286\,E^{-06}$
I_{Na} state O_1	O_{1Na}	$1.196\,E^{-08}$
I_{Na} state O_2	O_{2Na}	$2.160\,E^{-09}$
I_{Na} state CI_0	CI_{0Na}	$4.869\,E^{-01}$
I_{Na} state CI_1	CI_{1Na}	$2.625\,E^{-01}$
I_{Na} state CI_2	CI_{2Na}	$5.306\,E^{-02}$
I_{Na} state CI_3	CI_{3Na}	$4.768\,E^{-03}$
I_{Na} state CI_4	CI_{4Na}	$1.606\,E^{-04}$
I_{Na} state I	I_{Na}	$3.097\,E^{-04}$

Iyer et al
Human cardiac cell model
(67 Variables)

For fine tuning of the optimal parameter set, the output of the annealing algorithm is fed into a Neldar-Mead simplex search algorithm (in which only downhill moves are accepted). This approach has been shown to be superior in finding the absolute minimum of functions of several variables (Goffe, 1994).

Model equations and parameters

All rate constants are expressed in units of ms^{-1} unless otherwise noted. Similarly, all concentrations are expressed in mM unless otherwise noted.

Constants

See Tables 1–4.

Membrane currents

See Table 5.

Sodium current I_{Na}

$$I_{Na} = \bar{G}_{Na}(O_{1Na} + O_{2Na})(V - E_{Na}). \quad (1)$$

$$E_{Na} = \frac{RT}{F}\ln\left(\frac{[Na^+]_o}{[Na^+]_i}\right). \quad (2)$$

$$\frac{dC_{0Na}}{dt} = -(4\alpha + c_n)(C_{0Na}) + (\beta)(C_{1Na}) + (c_f)(CI_{0Na}). \quad (3)$$

$$\frac{dC_{1Na}}{dt} = -(\beta + c_n \cdot a + 3\alpha)(C_{1Na}) + (4\alpha)(C_{0Na}) + (2\beta)(C_{2Na}) + (c_f/a)(CI_{1Na}). \quad (4)$$

$$\frac{dC_{2Na}}{dt} = -(2\beta + c_n \cdot a^2 + 2\alpha)(C_{2Na}) + (3\alpha)(C_{1Na}) + (3\beta)(C_{3Na}) + (c_f/a^2)(CI_{2Na}). \quad (5)$$

$$\frac{dC_{3Na}}{dt} = -(3\beta + c_n \cdot a^3 + \alpha)(C_{3Na}) + (2\alpha)(C_{2Na}) + (4\beta)(C_{4Na}) + (c_f/a^3)(CI_{3Na}). \quad (6)$$

$$\frac{dC_{4Na}}{dt} = -(4\beta + c_n \cdot a^4 + \gamma + \eta)(C_{4Na}) + (\alpha)(C_{3Na}) + (\delta)(O_{1Na}) + (\nu)(O_{2Na}) + (c_f/a^4)(CI_{4Na}). \quad (7)$$

$$\frac{dO_{1Na}}{dt} = -(\delta + \varepsilon + o_n)(O_{1Na}) + (\gamma)(C_{4Na}) + (\omega)(O_{2Na}) + (o_f)(I_{Na}). \quad (8)$$

TABLE 1 Physical constants

Constant	Symbol	Value
Faraday's constant	F	96.5°C/mmol
Temperature	T	310 K
Gas constant	R	8.315 J/mol –K
Boltzmann's constant	K	1.381 E^{-23} J/K
Planck's constant	H	6.626 E^{-31} J/ms

TABLE 2 Cell geometry constants

Constant	Symbol	Value
Cell capacitance	A_{cap}	153.4 pF
Myoplasm volume	V_{myo}	25.84 E^{-6} μL
Junctional SR volume	V_{JSR}	0.16 E^{-6} μL
Network SR volume	V_{NSR}	2.1 E^{-6} μL
Subspace volume	V_{ss}	1.2 E^{-9} μL

$$\frac{dO_{2Na}}{dt} = -(\omega + \nu)(O_{2Na}) + (\varepsilon)(O_{1Na}) + (\eta)(C_{4Na}). \quad (9)$$

$$\frac{dCI_{0Na}}{dt} = -(c_f + 4\alpha a)(C_{3Na}) + (\beta/a)(CI_{1Na}) + (c_n)(C_{0Na}). \quad (10)$$

$$\frac{dCI_{1Na}}{dt} = -(\beta/a + 3\alpha a + c_f/a)(CI_{1Na}) + (4\alpha a)(CI_{0Na}) + (2\beta/a)(CI_{2Na}) + (c_n a)(C_{1Na}). \quad (11)$$

$$\frac{dCI_{2Na}}{dt} = -(2\beta/a + 2\alpha a + c_f/a^2)(CI_{2Na}) + (3\alpha a)(CI_{1Na}) + (3\beta/a)(CI_{3Na}) + (c_n a^2)(C_{2Na}). \quad (12)$$

$$\frac{dCI_{3Na}}{dt} = -(3\beta/a + \alpha a + c_f/a^3)(CI_{3Na}) + (2\alpha a)(CI_{2Na}) + (4\beta/a)(CI_{4Na}) + (c_n a^3)(C_{3Na}). \quad (13)$$

$$\frac{dCI_{4Na}}{dt} = -(4\beta/a + \gamma\gamma + c_f/a^4)(CI_{4Na}) + (\alpha a)(CI_{3Na}) + (\delta\delta)(I_{Na}) + (c_n a^4)(C_{4Na}). \quad (14)$$

$$\frac{dI_{Na}}{dt} = -(\delta\delta + o_f)(I_{Na}) + (\gamma\gamma)(CI_{4Na}) + (o_n)(O_{1Na}). \quad (15)$$

See Table 6.

Rapidly-activating delayed rectifier K^+ current I_{Kr}

$$I_{Kr} = \bar{G}_{Kr} f([K^+]_o)(O_{Kr})(V - E_K). \quad (16)$$

$$E_K = \frac{RT}{F}\ln\left(\frac{[K^+]_o}{[K^+]_i}\right). \quad (17)$$

$$f([K^+]_o) = \sqrt{\left(\frac{[K^+]_o}{4}\right)}. \quad (18)$$

$$\frac{dC_{1Kr}}{dt} = -(\alpha_0)(C_{1Kr}) + (\beta_0)(C_{2Kr}). \quad (19)$$

$$\frac{dC_{2Kr}}{dt} = -(\beta_0 + k_f)(C_{2Kr}) + (\alpha_0)(C_{1Kr}) + (k_b)(C_{3Kr}). \quad (20)$$

TABLE 3 Standard ionic concentrations

Permeant ion	Symbol	Value
Sodium	$[Na^+]_o$	138 mM
Potassium	$[K^+]_o$	4 mM
Calcium	$[Ca^{2+}]_o$	2 mM

$$\frac{dO_{Kr}}{dt} = -(\beta_1 + \alpha_i)(O_{Kr}) + (\alpha_1)(C_{3Kr}) + (\beta_i)(I_{Kr}). \quad (21)$$

$$\frac{dO_{Kr}}{dt} = -(\beta_1 + \alpha_i)(O_{Kr}) + (\alpha_1)(C_{3Kr}) + (\beta_i)(I_{Kr}). \quad (22)$$

$$\frac{dI_{Kr}}{dt} = -(\psi + \beta_i)(I_{Kr}) + (\alpha_{i3})(C_{3Kr}) + (\alpha_i)(O_{Kr}). \quad (23)$$

$$\psi = \frac{(\beta_1 \cdot \beta_i \cdot \alpha_{i3})}{(\alpha_1 \cdot \alpha_i)}. \quad (24)$$

See Table 7.

Slowly-activating delayed rectifier K^+ current I_{Ks}

$$I_{Ks} = \bar{G}_{Ks}(O_{1Ks} + O_{2Ks})(V - E_K). \quad (25)$$

$$E_K = \frac{RT}{F}\ln\left(\frac{[K^+]_o}{[K^+]_i}\right). \quad (26)$$

$$\frac{dC_{0Ks}}{dt} = -(\alpha)(C_{0Ks}) + (\beta)(C_{1Ks}). \quad (27)$$

$$\frac{dC_{1Ks}}{dt} = -(\beta + \gamma)(C_{1Ks}) + (\alpha)(C_{0Ks}) + (\delta)(O_{1Ks}). \quad (28)$$

$$\frac{dO_{1Ks}}{dt} = -(\delta + \varepsilon)(O_{1Ks}) + (\gamma)(C_{1Ks}) + (\omega)(O_{2Ks}). \quad (29)$$

$$\frac{dO_{2Ks}}{dt} = -(\omega)(O_{2Ks}) + (\varepsilon)(O_{1Ks}). \quad (30)$$

See Table 8.

Transient outward K^+ current I_{to1}

Fast recovering component, Kv4.3

$$I_{Kv4.3} = \bar{G}_{Kv4.3}(O_{Kvf})(V - E_K). \quad (31)$$

$$E_K = \frac{RT}{F}\ln\left(\frac{[K^+]_o}{[K^+]_i}\right). \quad (32)$$

TABLE 5 Time-dependent current densities

Current	Symbol	Density
Sodium current	G_{Na}	56.32 mS/μF
Delayed rectifier, rapid component	G_{Kr}	0.0186 mS/μF
Delayed rectifier, slow component	G_{Ks}	0.0035 mS/μF
Transient outward current, fast recovery	$G_{Kv4.3}$	0.0775 mS/μF
Transient outward current, slow recovery	$P_{Kv1.4}$	4.161 d^{-8} cm/s

$$\frac{dC_{0Kvf}}{dt} = -(4\alpha_a + \beta_i)(C_{0Kvf}) + (\beta_a)(C_{1Kvf}) + (\alpha_i)(CI_{0Kvf}). \quad (33)$$

$$\frac{dC_{1Kvf}}{dt} = -(\beta_a + 3\alpha_a + f_1\beta_i)(C_{1Kvf}) + (4\alpha_a)(C_{0Kvf}) + (2\beta_a)(C_{2Kvf}) + (\alpha_i/b_1)(CI_{1Kvf}). \quad (34)$$

$$\frac{dC_{2Kvf}}{dt} = -(2\beta_a + 2\alpha_a + f_2\beta_i)(C_{2Kvf}) + (3\alpha_a)(C_{1Kvf}) + (3\beta_a)(C_{3Kvf}) + (\alpha_i/b_2)(CI_{2Kvf}). \quad (35)$$

$$\frac{dC_{3Kvf}}{dt} = -(3\beta_a + \alpha_a + f_3\beta_i)(C_{3Kvf}) + (2\alpha_a)(C_{2Kvf}) + (4\beta_a)(C_{4Kvf}) + (\alpha_i/b_3)(CI_{3Kvf}). \quad (36)$$

$$\frac{dO_{Kvf}}{dt} = -(4\beta_a + f_4\beta_i)(O_{Kvf}) + (\alpha_a)(C_{3Kvf}) + (\alpha_i/b_4)(OI_{Kvf}). \quad (37)$$

$$\frac{dCI_{0Kvf}}{dt} = -(b_1 4\alpha_a + a_i)(CI_{0Kvf}) + (\beta_a/f_1)(CI_{1Kvf}) + (\beta_i)(C_{0Kvf}). \quad (38)$$

TABLE 6 I_{Na} rate constants

	$\lambda = Q\frac{kT}{h}\exp\left(\frac{-\Delta H_\lambda}{RT} + \frac{\Delta S_\lambda}{R} + \frac{z_\lambda FV}{RT}\right)$ parameters		
Rate constant	ΔH, J/mol	ΔS, J/mol –K	z
α	114,007	224.114	0.2864
β	272,470	708.146	–2.2853
γ	196,337	529.952	2.7808
δ	133,690	229.205	–1.5580
O_n	62,123	39.295	0.2888
O_f	97,658	1.510	0.0685
$\gamma\gamma$	–116,431	–578.317	0.7641
$\delta\delta$	55,701	–130.639	–3.6498
ε	85,800	70.078	0
ω	121,955	225.175	0
η	147,814	338.915	2.1360
ν	121,322	193.265	–1.7429
C_n	287,913	786.217	0
C_f	59,565	0.00711	0
Scaling a	1.4004		
Q	1.389		

TABLE 7 I_{Kr} **rate constants**

Rate constant	Value
α_o	$0.0171 \cdot \exp(0.0330\ V)\ ms^{-1}$
β_o	$0.0397 \cdot \exp(-0.0431\ V)\ ms^{-1}$
α_1	$0.0206 \cdot \exp(0.0262\ V)\ ms^{-1}$
β_1	$0.0013 \cdot \exp(-0.0269\ V)\ ms^{-1}$
α_i	$0.1067 \cdot \exp(0.0057\ V)\ ms^{-1}$
β_i	$0.0065 \cdot \exp(-0.0454\ V)\ ms^{-1}$
α_{i3}	$8.04\ E^{-5} \cdot \exp(6.98\ E^{-7}\ V)\ ms^{-1}$
k_f	$0.0261\ ms^{-1}$
k_b	$0.1483\ ms^{-1}$

$$\frac{dCI_{1Kvf}}{dt} = -(\beta_a/f_1 + b_2 3\alpha_a/b_1 + \alpha_i/b_1)(CI_{1Kvf}) + (b_1 4\alpha_a)(CI_{0Kvf}) + (f_1 2\beta_a/f_2)(CI_{2Kvf}) + (f_1\beta_i)(C_{1Kvf}). \quad (39)$$

$$\frac{dCI_{2Kvf}}{dt} = -(f_1 2\beta_a/f_2 + b_3 2\alpha_a/b_2 + \alpha_i/b_2)(CI_{2Kvf}) + (b_2 3\alpha_a/b_1)(CI_{1Kvf}) + (f_2 3\beta_a/f_3)(CI_{3Kvf}) + (f_2\beta_i)(C_{2Kvf}). \quad (40)$$

$$\frac{dCI_{3Kvf}}{dt} = -(f_2 3\beta_a/f_3 + b_4\alpha_a/b_3 + \alpha_i/b_3)(CI_{3Kvf}) + (b_3 2\alpha_a/b_2)(CI_{2Kvf}) + (f_3 4\beta_a/f_4)(OI_{Kvf}) + (f_3\beta_i)(C_{3Kvf}). \quad (41)$$

$$\frac{dOI_{Kvf}}{dt} = -(f_3 4\beta_a/f_4 + \alpha_i/b_4)(OI_{Kvf}) + (b_4\alpha_a/b_3) \times (CI_{3Kvf}) + (f_4\beta_i)(O_{Kvf}). \quad (42)$$

Slowly recovering component, Kv *1.4*

$$I_{Kv1.4} = P_{Kv1.4} O_{Kvs} \frac{4VF^2}{RT} \frac{[K^+]_i \exp\left(\frac{VF}{RT}\right) - [K^+]_o}{\exp\left(\frac{VF}{RT}\right) - 1} + I_{Kv1.4,Na}. \quad (43)$$

$$I_{Kv1.4,Na} = 0.02 \cdot P_{Kv1.4} O_{Kvs} \frac{4VF^2}{RT} \frac{[Na^+]_i \exp\left(\frac{VF}{RT}\right) - [Na^+]_o}{\exp\left(\frac{VF}{RT}\right) - 1}. \quad (44)$$

TABLE 8 I_{Ks} **rate constants**

Rate constant	Value
α	$7.956\ E^{-3}\ ms^{-1}$
β	$2.16\ E^{-1} \cdot \exp(-0.00002\ V)\ ms^{-1}$
γ	$3.97\ E^{-2}\ ms^{-1}$
δ	$7\ E^{-3} \cdot \exp(-0.15\ V)\ ms^{-1}$
ε	$7.67\ E^{-3} \cdot \exp(0.087\ V)\ ms^{-1}$
ω	$3.80\ E^{-3} \cdot \exp(-0.014\ V)\ ms^{-1}$

$$\frac{dC_{0Kvs}}{dt} = -(4\alpha_a + \beta_i)(C_{0Kvs}) + (\beta_a)(C_{1Kvs}) + (\alpha_i)(CI_{0Kvs}). \quad (45)$$

$$\frac{dC_{1Kvs}}{dt} = -(\beta_a + 3\alpha_a + f_1\beta_i)(C_{1Kvs}) + (4\alpha_a)(C_{0Kvs}) + (2\beta_a)(C_{2Kvs}) + (\alpha_i/b_1)(CI_{1Kvs}). \quad (46)$$

$$\frac{dC_{2Kvs}}{dt} = -(2\beta_a + 2\alpha_a + f_2\beta_i)(C_{2Kvs}) + (3\alpha_a)(C_{1Kvs}) + (3\beta_a)(C_{3Kvs}) + (\alpha_i/b_2)(CI_{2Kvs}). \quad (47)$$

$$\frac{dC_{3Kvs}}{dt} = -(3\beta_a + \alpha_a + f_3\beta_i)(C_{3Kvs}) + (2\alpha_a)(C_{2Kvs}) + (4\beta_a)(C_{4Kvs}) + (\alpha_i/b_3)(CI_{3Kvs}). \quad (48)$$

$$\frac{dO_{Kvs}}{dt} = -(4\beta_a + f_4\beta_i)(O_{Kvs}) + (\alpha_a)(C_{3Kvs}) + (\alpha_i/b_4)(OI_{Kvs}). \quad (49)$$

$$\frac{dCI_{0Kvs}}{dt} = -(b_1 4\alpha_a + a_i)(CI_{0Kvs}) + (\beta_a/f_1)(CI_{1Kvs}) + (\beta_i)(C_{0Kvs}). \quad (50)$$

$$\frac{dCI_{1Kvs}}{dt} = -(\beta_a/f_1 + b_2 3\alpha_a/b_1 + \alpha_i/b_1)(CI_{1Kvs}) + (b_1 4\alpha_a)(CI_{0Kvs}) + (f_1 2\beta_a/f_2)(CI_{2Kvs}) + (f_1\beta_i)(C_{1Kvs}). \quad (51)$$

$$\frac{dCI_{2Kvs}}{dt} = -(f_1 2\beta_a/f_2 + b_3 2\alpha_a/b_2 + \alpha_i/b_2)(CI_{2Kvs}) + (b_2 3\alpha_a/b_1)(CI_{1Kvs}) + (f_2 3\beta_a/f_3)(CI_{3Kvs}) + (f_2\beta_i)(C_{2Kvs}). \quad (52)$$

$$\frac{dCI_{3Kvs}}{dt} = -(f_2 3\beta_a/f_3 + b_4\alpha_a/b_3 + \alpha_i/b_3)(CI_{3Kvs}) + (b_3 2\alpha_a/b_2)(CI_{2Kvs}) + (f_3 4\beta_a/f_4)(OI_{Kvs}) + (f_3\beta_i)(C_{3Kvs}). \quad (53)$$

$$\frac{dOI_{Kvs}}{dt} = -(f_3 4\beta_a/f_4 + \alpha_i/b_4)(OI_{Kvs}) + (b_4\alpha_a/b_3)(CI_{3Kvs}) + (f_4\beta_i)(O_{Kvs}). \quad (54)$$

See Table 9.

Time-independent K^+ current I_{K1}

$$I_{K1} = \bar{G}_{K1} K_1^{\infty}(V)\left(\sqrt{[K^+]_o}\right)(V - E_K). \quad (55)$$

TABLE 9 I_{to1} **rate constants**

Rate constant	$Kv4.3$ current, ms^{-1}	$Kv1.4$ current, ms^{-1}
α_a	$0.675{,}425 \cdot \exp(0.0255\ V)$	$1.840024 \cdot \exp(0.0077\ V)$
β_a	$0.088269 \cdot \exp(-0.0883\ V)$	$0.010817 \cdot \exp(-0.0779\ V)$
α_i	0.109566	0.003058
β_i	$3.03334\ E^{-4}$	$2.4936\ E^{-6}$
f_1	1.66120	0.52465
f_2	22.2463	17.5188
f_3	195.978	938.587
f_4	181.609	54749.1
b_1	0.72246	1.00947
b_2	0.47656	1.17100
b_3	7.77537	0.63902
b_4	318.232	2.12035

$$K_1^{\infty}(V) = \frac{1}{0.94 + \exp\left(\frac{1.26}{RT/F}(V - EK)\right)}. \quad (56)$$

$$E_K = \frac{RT}{F}\ln\left(\frac{[K^+]_o}{[K^+]_i}\right). \quad (57)$$

$$\bar{G}_{K1} = 0.125 \frac{mS}{\mu F \cdot mM^{1/2}}. \quad (58)$$

Sodium handling mechanisms

NCX current I_{NaCa}

$$I_{NaCa} = k_{NaCa} \frac{1}{K_{m,Na}^3 + [Na^+]_o^3} \frac{1}{K_{m,Ca} + [Ca^{2+}]_o} \frac{1}{1 + k_{sat} e^{(\eta - 1)\frac{VF}{RT}}} \times \left(e^{\frac{\eta VF}{RT}} [Na^+]_i^3 [Ca^{2+}]_o - e^{\frac{(\eta - 1)VF}{RT}} [Na^+]_o^3 [Ca^{2+}]_i\right). \quad (59)$$

Na^+ background current $I_{Na,b}$

$$I_{Na,b} = \bar{G}_{Na,b}(V - E_{Na}). \quad (60)$$

Na^+-K^+ pump current I_{NaK}

$$I_{NaK} = k_{NaK} f_{NaK} \frac{1}{1 + \left(\frac{K_{m,Nai}}{[Na^+]_i}\right)^{1.5}} \frac{[K^+]_o}{[K^+]_o + K_{m,Ko}}. \quad (61)$$

$$f_{NaK} = \frac{1}{1 + 0.1245 e^{-0.1\frac{VF}{RT}} + 0.0365 \sigma e^{-1.33\frac{VF}{RT}}}. \quad (62)$$

$$\sigma = \frac{1}{7}\left(e^{\frac{[Na^+]_o}{67.3}} - 1\right). \quad (63)$$

See Table 10.

TABLE 10 Sodium handling parameters

Parameter	Value
$G_{Na,b}$	$0.001\ mS/\mu F$
$K_{m,Na}$	87.5 mM
$K_{m,Ca}$	1.38 mM
k_{sat}	0.2
η	0.35
k_{NaK}	$2.387\ \mu A/\mu F$
$K_{m,Nai}$	20 mM
$K_{m,Ko}$	1.5 mM

Calcium handling mechanisms

Sarcolemmal Ca^{2+} pump current $I_{p(Ca)}$

$$I_{p(Ca)} = \bar{I}_{p(Ca)} \frac{[Ca^{2+}]_i}{K_{m,p(Ca)} + [Ca^{2+}]_i}. \quad (64)$$

Ca^{2+} background current $I_{Ca,b}$

$$I_{Ca,b} = \bar{G}_{Ca,b}(V - E_{Ca}). \quad (65)$$

$$E_{Ca} = \frac{RT}{2F}\ln\left(\frac{[Ca^{2+}]_o}{[Ca^{2+}]_i}\right). \quad (66)$$

See Table 11.

L-type Ca^{2+} current I_{Ca}

$$\alpha = 1.997 e^{0.012(V-35)}. \quad (67)$$

$$\beta = 0.0882 e^{-0.065(V-22)}. \quad (68)$$

$$\alpha' = \alpha a. \quad (69)$$

$$\beta' = \frac{\beta}{b}. \quad (70)$$

$$\gamma = 0.0554[Ca^{2+}]_{ss}. \quad (71)$$

$$\frac{dC_{0L}}{dt} = -(4\alpha + \gamma)C_{0L} + \beta C_{1L} + \omega C_{Ca0L}. \quad (72)$$

$$\frac{dC_{1L}}{dt} = -(3\alpha + \beta + \gamma a)C_{1L} + 4\alpha C_{0L} + 2\beta C_{2L} + \frac{\omega}{b} C_{Ca1L}. \quad (73)$$

$$\frac{dC_{2L}}{dt} = -(2\alpha + 2\beta + \gamma a^2)C_{2L} + 3\alpha C_{1L} + 3\beta C_{3L} + \frac{\omega}{b^2} C_{Ca2L}. \quad (74)$$

$$\frac{dC_{3L}}{dt} = -(\alpha + 3\beta + \gamma a^3)C_{3L} + 2\alpha C_{2L} + 4\beta C_{4L} + \frac{\omega}{b^3} C_{Ca3L}. \quad (75)$$

$$\frac{dC_{4L}}{dt} = -(f + 4\beta + \gamma a^4)C_{4L} + \alpha C_{3L} + g O_L + \frac{\omega}{b^4} C_{Ca4L}. \quad (76)$$

TABLE 11 Membrane calcium exchangers, background current

Parameter	Value
$\bar{I}_{p(Ca)}$	0.05 pA/pF
$K_{m,p(Ca)}$	0.0005 mM
$\bar{G}_{Ca,b}$	7.684 d^{-5} ms/μF

$$\frac{dO_L}{dt} = -gO_L + fC_{4L}. \quad (77)$$

$$\frac{dC_{Ca0L}}{dt} = -(4\alpha' + \omega)C_{Ca0L} + \beta' C_{Ca1L} + \gamma C_{0L}. \quad (78)$$

$$\frac{dC_{Ca1L}}{dt} = -\left(3\alpha' + \beta' + \frac{\omega}{b}\right)C_{Ca1L} + 4\alpha' C_{Ca0L} + 2\beta' C_{Ca2L} + \gamma a C_{1L}. \quad (79)$$

$$\frac{dC_{Ca2L}}{dt} = -\left(2\alpha' + 2\beta' + \frac{\omega}{b^2}\right)C_{Ca2L} + 3\alpha' C_{Ca1L} + 3\beta' C_{Ca3L} + \gamma a^2 C_{2L}. \quad (80)$$

$$\frac{dC_{Ca3L}}{dt} = -\left(\alpha' + 3\beta' + \frac{\omega}{b^3}\right)C_{Ca3L} + 2\alpha' C_{Ca2L} + 4\beta' C_{Ca4L} + \gamma a^3 C_{3L}. \quad (81)$$

$$\frac{dC_{Ca4L}}{dt} = -\left(4\beta' + \frac{\omega}{b^4}\right)C_{Ca4L} + \alpha' C_{Ca3L} + \gamma a^4 C_{4L}. \quad (82)$$

$$\frac{dy_{Ca}}{dt} = \frac{y_\infty - y}{\tau_y}. \quad (83)$$

$$y_\infty = \frac{0.82}{1 + e^{\frac{V+28.5}{7.8}}} + 0.18. \quad (84)$$

$$\tau_y = \frac{1}{\frac{0.00653}{0.5 + e^{-V/7.1}} + 0.00512e^{-V/39.8}} \quad (85)$$

$$\bar{I}_{Ca} = \frac{\bar{P}_{Ca}}{C_{sc}}\frac{4VF^2}{RT}\frac{0.001e^{2VF/RT} - 0.341[Ca^{2+}]_o}{e^{2VF/RT} - 1}. \quad (86)$$

$$I_{Ca} = \bar{I}_{Ca} y O_L \quad (87)$$

$$I_{Ca,K} = \frac{P'_K}{C_{SC}} y O_L \left(\frac{VF^2}{RT}\frac{[K^+]_i e^{\frac{VF}{RT}} - [K^+]_o}{e^{\frac{VF}{RT}} - 1}\right). \quad (88)$$

$$P'_K = \frac{\bar{P}_K}{1 + \frac{\bar{I}_{Ca}}{I_{Ca,half}}} \quad (89)$$

See Table 12.

RyR channel

$$\frac{dP_{C1}}{dt} = -k_a^+[Ca^{2+}]_{ss}^n P_{C1} + k_a^- P_{O1}. \quad (90)$$

TABLE 12 I_{Ca} parameters

Parameter	Value
f	0.3 ms^{-1}
g	4 ms^{-1}
a	2
b	2
ω	2.5 d^{-3} ms^{-1} mm^{-1}
P_{Ca}	1.7283 d^{-3} cm/s
P_K	3.2018 d^{-6} cm/s
$I_{Ca,half}$	−0.265 pA/pF

$$\frac{dP_{O1}}{dt} = k_a^+[Ca^{2+}]_{ss}^n P_{C1} - k_a^- P_{O1} - k_b^+[Ca^{2+}]_{ss}^m P_{O1} + k_b^- P_{O2} - k_c^+ P_{O1} + k_c^- P_{C2}. \quad (91)$$

$$\frac{dP_{O2}}{dt} = k_b^+[Ca^{2+}]_{ss}^m P_{O1} - k_b^- P_{O2}. \quad (92)$$

$$\frac{dP_{C2}}{dt} = k_c^+ P_{O1} - k_c^- P_{C2}. \quad (93)$$

$$J_{rel} = v_1(P_{O1} + P_{O2})([Ca^{2+}]_{JSR} - [Ca^{2+}]_{SS}). \quad (94)$$

SERCA2a pump

$$f_b = \left(\frac{[Ca^{2+}]_i}{K_{fb}}\right)^{N_{fb}}. \quad (95)$$

$$r_b = \left(\frac{[Ca^{2+}]_{NSR}}{K_{rb}}\right)^{N_{rb}}. \quad (96)$$

$$J_{up} = K_{SR}\left(\frac{v_{maxf} f_b - v_{maxr} r_b}{1 + f_b + r_b}\right). \quad (97)$$

See Table 13.

Intracellular Ca^{2+} fluxes

$$J_{tr} = \frac{[Ca^{2+}]_{NSR} - [Ca^{2+}]_{JSR}}{\tau_{tr}}. \quad (98)$$

TABLE 13 *SR* parameters

Parameter	Value
K_a^+	0.01215 μM^{-4} ms^{-1}
K_a^-	0.576 ms^{-1}
K_b^+	0.00405 μM^{-3} ms^{-1}
K_b^-	1.93 ms^{-1}
K_c^+	0.3 ms^{-1}
K_c^-	0.0009 ms^{-1}
v_1	1.8 ms^{-1}
K_{fb}	0.000168 mM
N_{fb}	1.2
K_{rb}	3.29 mM
N_{rb}	1
v_{maxf}	0.0748 d^{-3} mM/ms
v_{maxr}	0.03748 d^{-3} mM/ms
K_{SR}	1.2

$$J_{xfer} = \frac{[Ca^{2+}]_{ss} - [Ca^{2+}]_i}{\tau_{xfer}}. \quad (99)$$

$$J_{trpn} = \frac{d[HTRPN_{Ca}]}{dt} + \frac{d[LTRPN_{Ca}]}{dt}. \quad (100)$$

$$\frac{d[HTRPN_{Ca}]}{dt} = k_{htrpn}^+[Ca^{2+}]_i([HTRPN]_{tot} - [HTRPN_{Ca}]) - k_{htrpn}^-[HTRPN_{Ca}]. \quad (101)$$

$$\frac{d[LTRPN_{Ca}]}{dt} = k_{ltrpn}^+[Ca^{2+}]_i([LTRPN]_{tot} - [LTRPN_{Ca}]) - k_{ltrpn}^-[LTRPN_{Ca}]. \quad (102)$$

See Table 14.

Intracellular ion concentrations and membrane potential

$$\frac{d[Na^+]_i}{dt} = -(I_{Na} + I_{Na,b} + 3I_{NaCa} + 3I_{NaK} + I_{Kv1.4,Na})\frac{A_{cap}C_{sc}}{V_{myo}F}. \quad (103)$$

$$\frac{d[K^+]_i}{dt} = -(I_{Kr} + I_{Ks} + I_{Kv4.3} + I_{Kv1.4,K} + I_{K1} + I_{Ca,K} - 2I_{NaK} + I_{stim})\frac{A_{cap}C_{sc}}{V_{myo}F}. \quad (104)$$

$$\frac{d[Ca^{2+}]_i}{dt} = \beta_i\left(J_{xfer} - J_{up} - J_{trpn} - (I_{Ca,b} - 2I_{NaCa} + I_{p(Ca)}) \times \frac{A_{cap}C_{sc}}{2V_{myo}F}\right). \quad (105)$$

$$\beta_i = \left(1 + \frac{[CMDN]_{tot}K_m^{CMDN}}{(K_m^{CMDN} + [Ca^{2+}]_i)^2} + \frac{[EGTA]_{tot}K_m^{EGTA}}{(K_m^{EGTA} + [Ca^{2+}]_i)^2}\right). \quad (106)$$

$$\beta_{ss} = \left(1 + \frac{[CMDN]_{tot}K_m^{CMDN}}{(K_m^{CMDN} + [Ca^{2+}]_{ss})^2} + \frac{[EGTA]_{tot}K_m^{EGTA}}{(K_m^{EGTA} + [Ca^{2+}]_{ss})^2}\right). \quad (107)$$

TABLE 14 Calcium buffering and diffusion

Parameter	Value
τ_{tr}	0.5747 ms
τ_{xfer}	26.7 ms
$HTRPN_{tot}$	140 d^{-3} mM
$LTRPN_{tot}$	70 d^{-3} mM
K_{HTRPN}^+	20 mM^{-1} ms^{-1}
K_{HTRPN}^-	0.066 d^{-3} ms^{-1}
K_{LTRPN}^+	40 mM^{-1} ms^{-1}
K_{LTRPN}^-	40 d^{-3} ms^{-1}
K_m^{CMDN}	2.38 d^{-3} mM
K_m^{CSQN}	0.8 mM
K_m^{EGTA}	1.5 d^{-4} mM
$EGTA_{tot}$	0 mM

$$\beta_{JSR} = \left(1 + \frac{[CSQN]_{tot}K_m^{CSQN}}{(K_m^{CSQN} + [Ca^{2+}]_{JSR})^2}\right)^{-1}. \quad (108)$$

$$\frac{d[Ca^{2+}]_{ss}}{dt} = \beta_{ss}\left(J_{rel}\frac{V_{JSR}}{V_{ss}} - J_{xfer}\frac{V_{myo}}{V_{ss}} - (I_{Ca})\frac{A_{cap}C_{sc}}{2V_{ss}F}\right). \quad (109)$$

$$\frac{d[Ca^{2+}]_{JSR}}{dt} = \beta_{JSR}(J_{tr} - J_{rel}). \quad (110)$$

$$\frac{d[Ca^{2+}]_{NSR}}{dt} = J_{up}\frac{V_{myo}}{V_{NSR}} - J_{tr}\frac{V_{JSR}}{V_{NSR}}. \quad (111)$$

$$\frac{dV}{dt} = -(I_{Na} + I_{Ca} + I_{Ca,K} + I_{Kr} + I_{Ks} + I_{K1} + I_{NaCa} + I_{NaK} + I_{Kv1.4} + I_{Kv4.3} + I_{p(Ca)} + I_{Ca,b} + I_{Na,b} + I_{stim}). \quad (112)$$

$$I_{stim} = -100\ \text{pA/pF}. \quad (113)$$

Cell Electrophysiology and Waves in Tissue

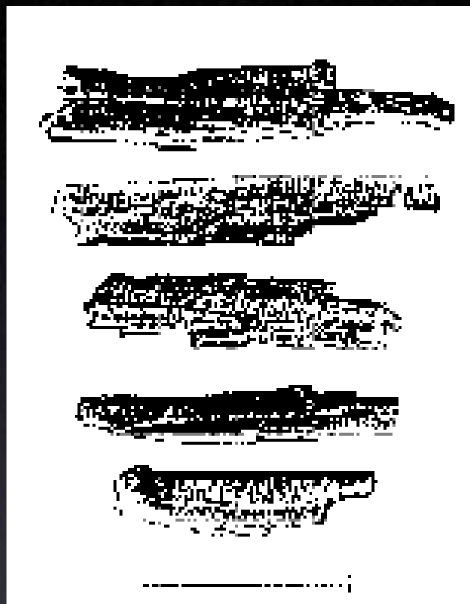

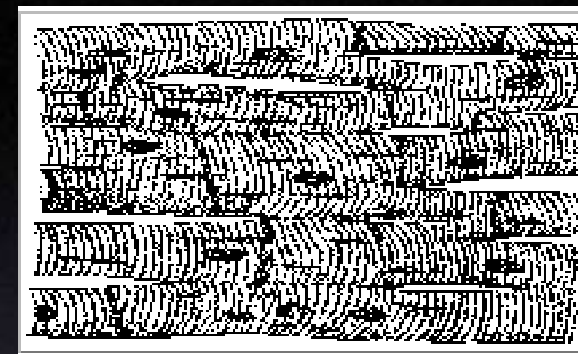

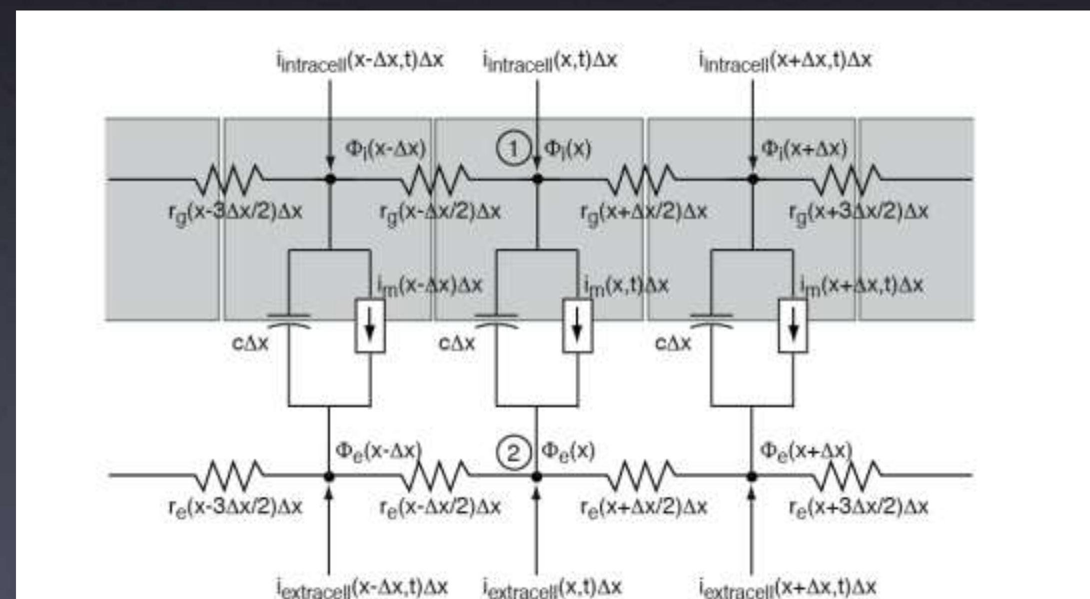

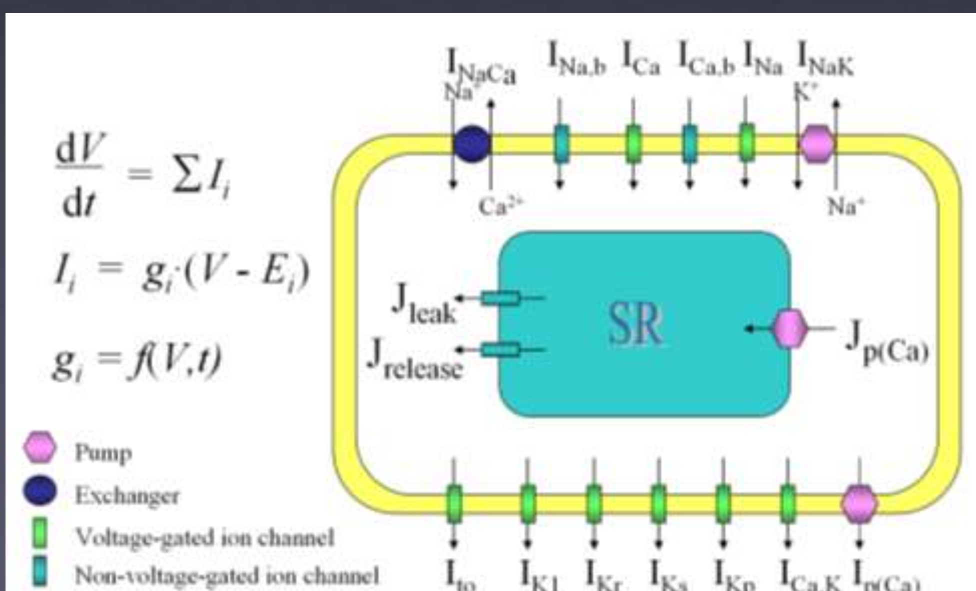

Electrical Waves in Tissue

Cells connected
in a 2D preparation

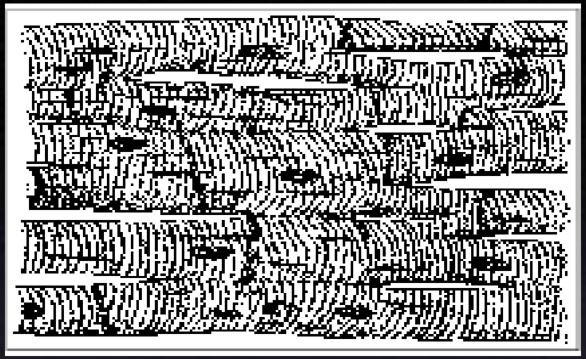

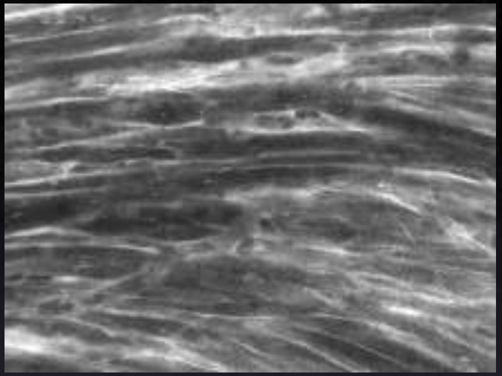

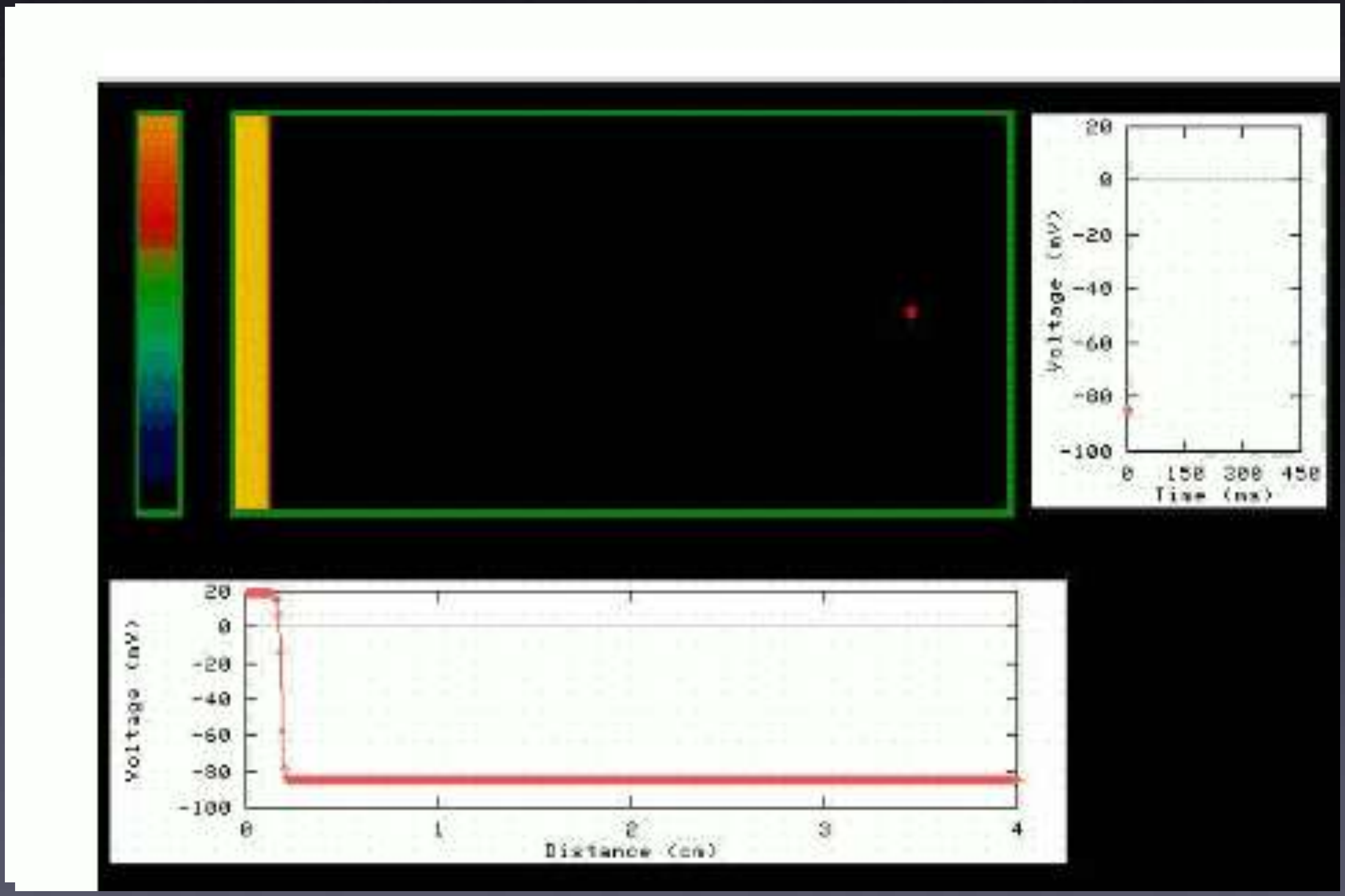

Normal Sinus Rhythm

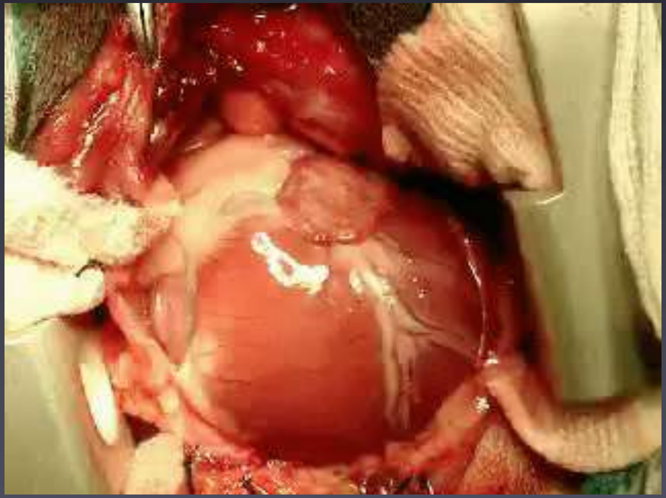

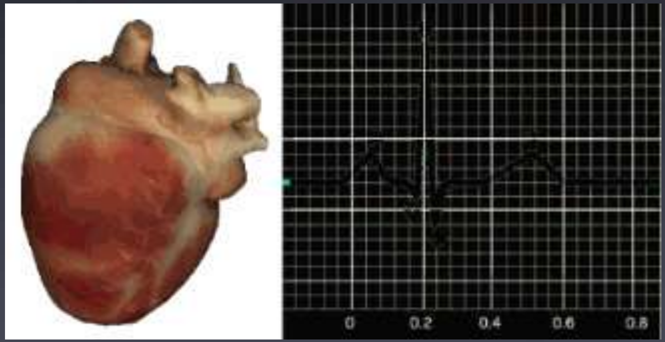

Ventricular Structure

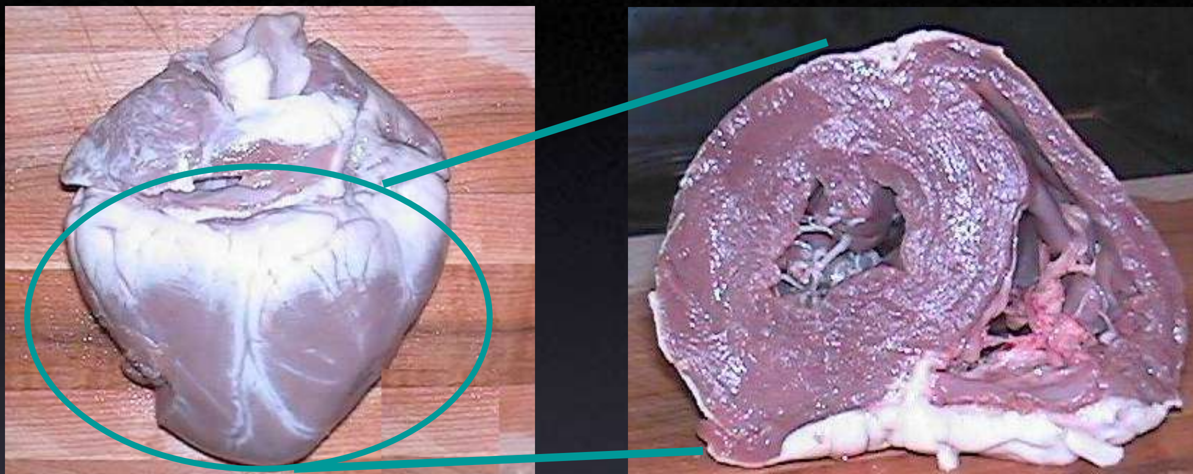

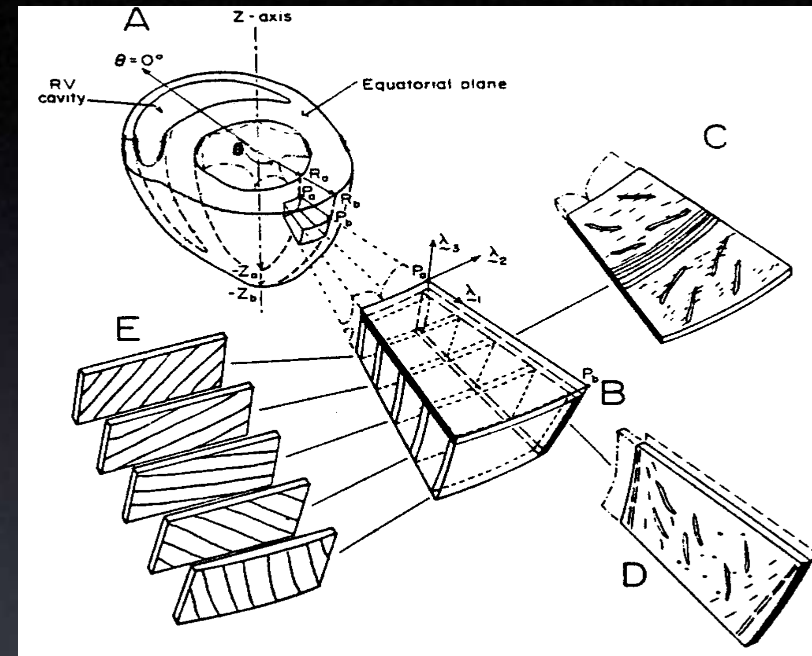

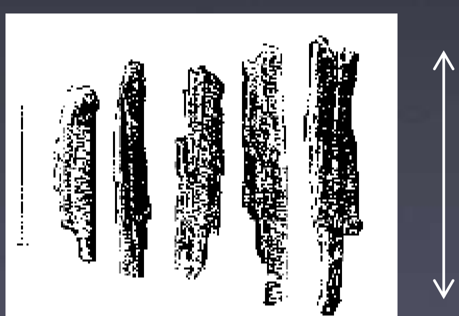

150μm

$D_{\parallel} : D_{\perp}$

10 : 1

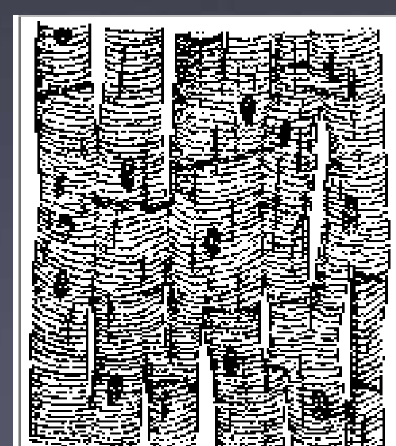

Ventricular Structure

Rabbit

Porcine

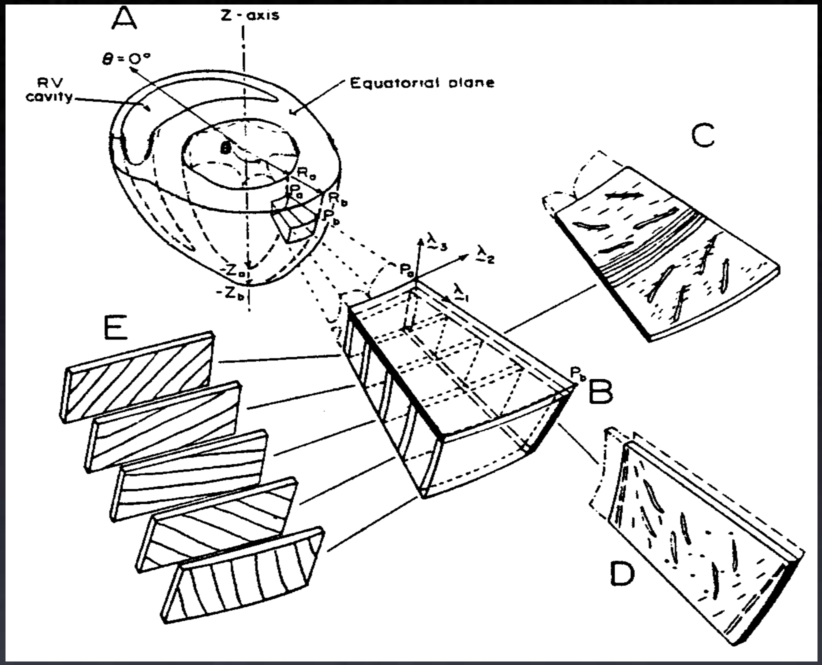

Canine

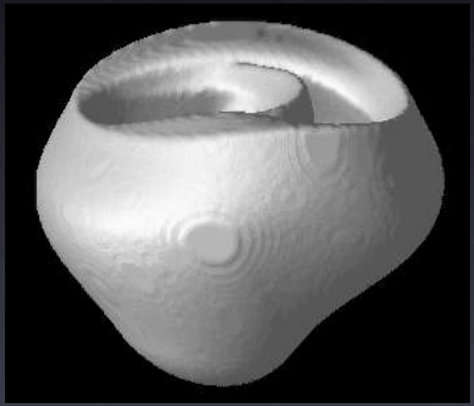

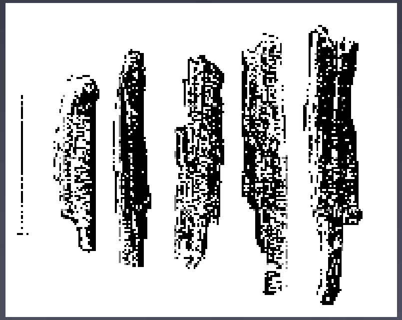

150μm

$D_{\parallel} : D_{\perp}$

10 : 1

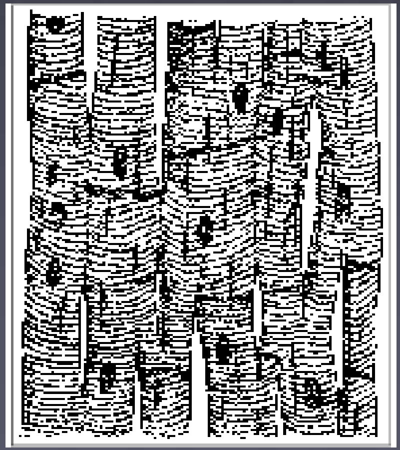

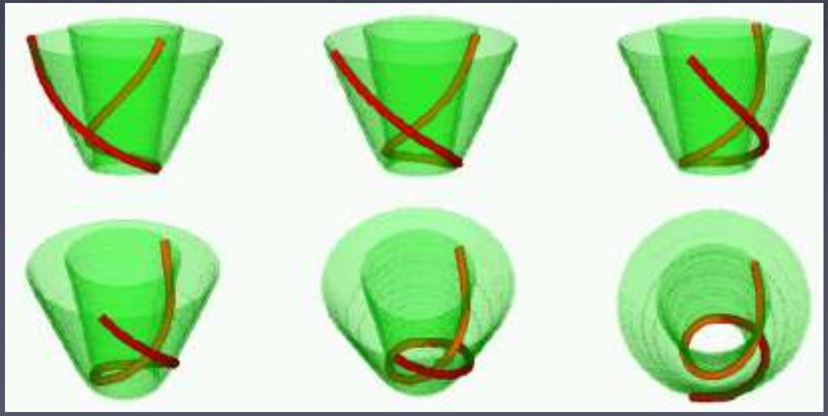

Atrial Structure

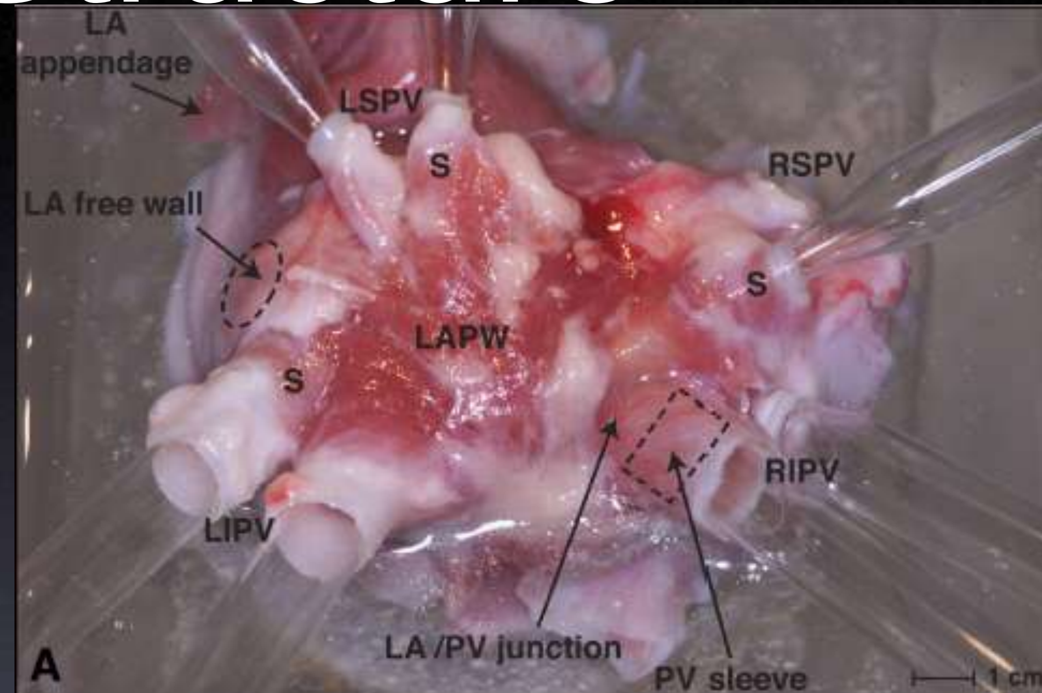

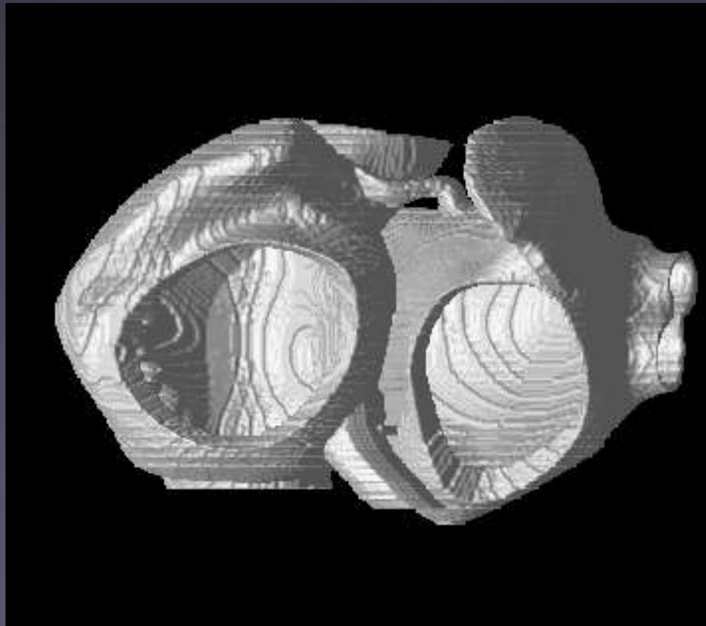

Visualization of Electrical Activity in the Heart

Visualizing Electrical Activity

- Computer simulations.
  - Mathematical models of cellular electrophysiology.
- Optical mapping.
  - Fluorescence recordings using voltage-sensitive dyes.
  - Intensity proportional to membrane potential.

Normal Sinus Rhythm
Plane Waves (Optical Mapping)

Electrical activity in the atria

Electrical activity in the ventricle

Spiral Waves in the Heart

Induction of Spiral Waves

Spiral (reentrant) waves can be initiated when tissue has repolarized nearly, but not fully, to the rest state.

Induction of Spiral Waves

Spiral (reentrant) waves can be initiated when tissue has repolarized nearly, but not fully, to the

e.

s all ming

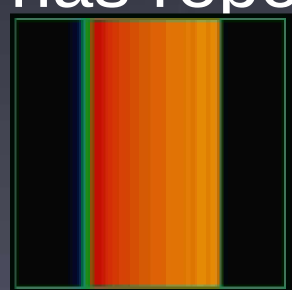

Too late

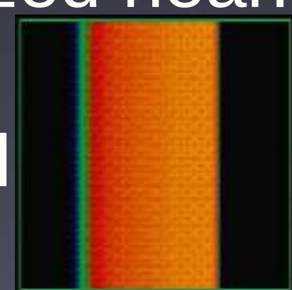

Too early

Just right!

There is a vulnerable window of time for initiation.

Reentrant Spiral Waves: Simulation

Fenton FH et al. Chaos 2002; 12, 852-892.

Reentrant Spiral Waves: Simulation

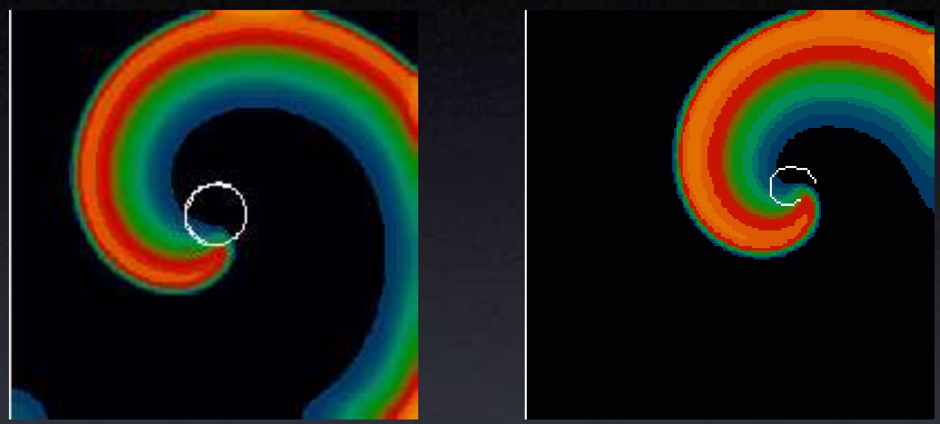

Fenton FH et al. Chaos 2002; 12, 852-892.

Reentrant Spiral Waves: Simulation

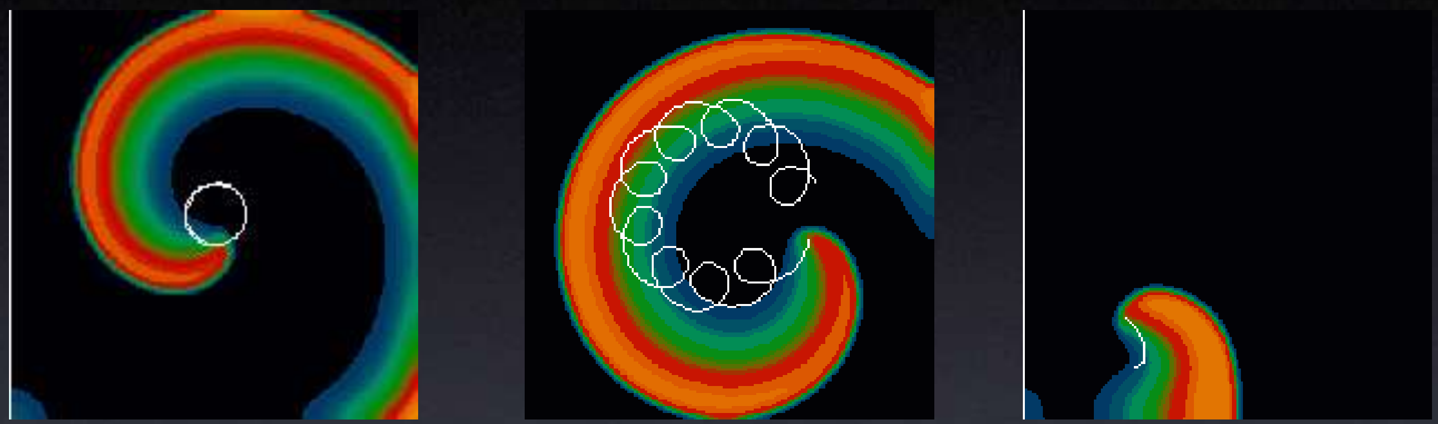

Fenton FH et al. Chaos 2002; 12, 852-892.

Reentrant Spiral Waves: Simulation

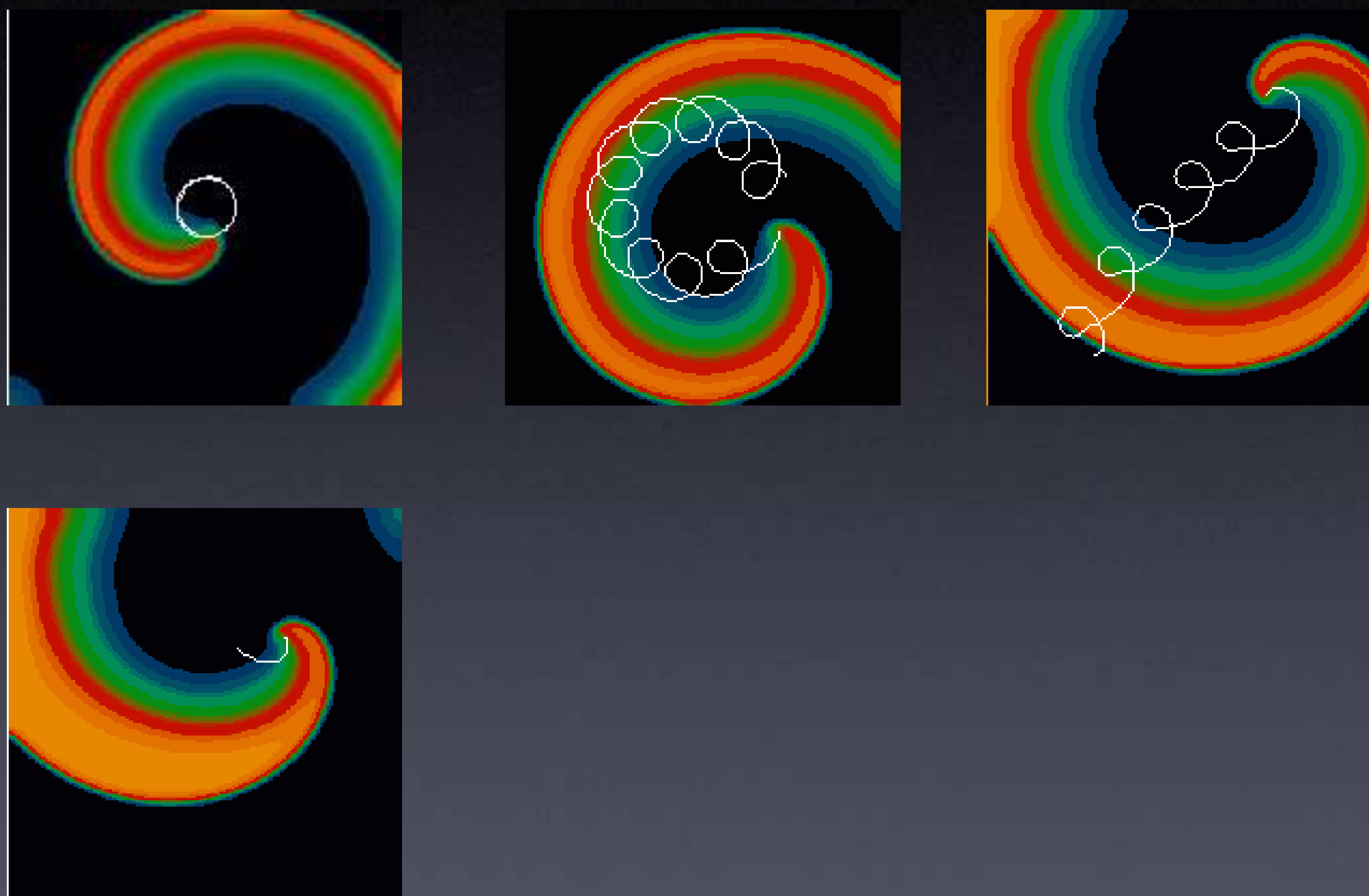

Fenton FH et al. Chaos 2002; 12, 852-892.

Reentrant Spiral Waves: Simulation

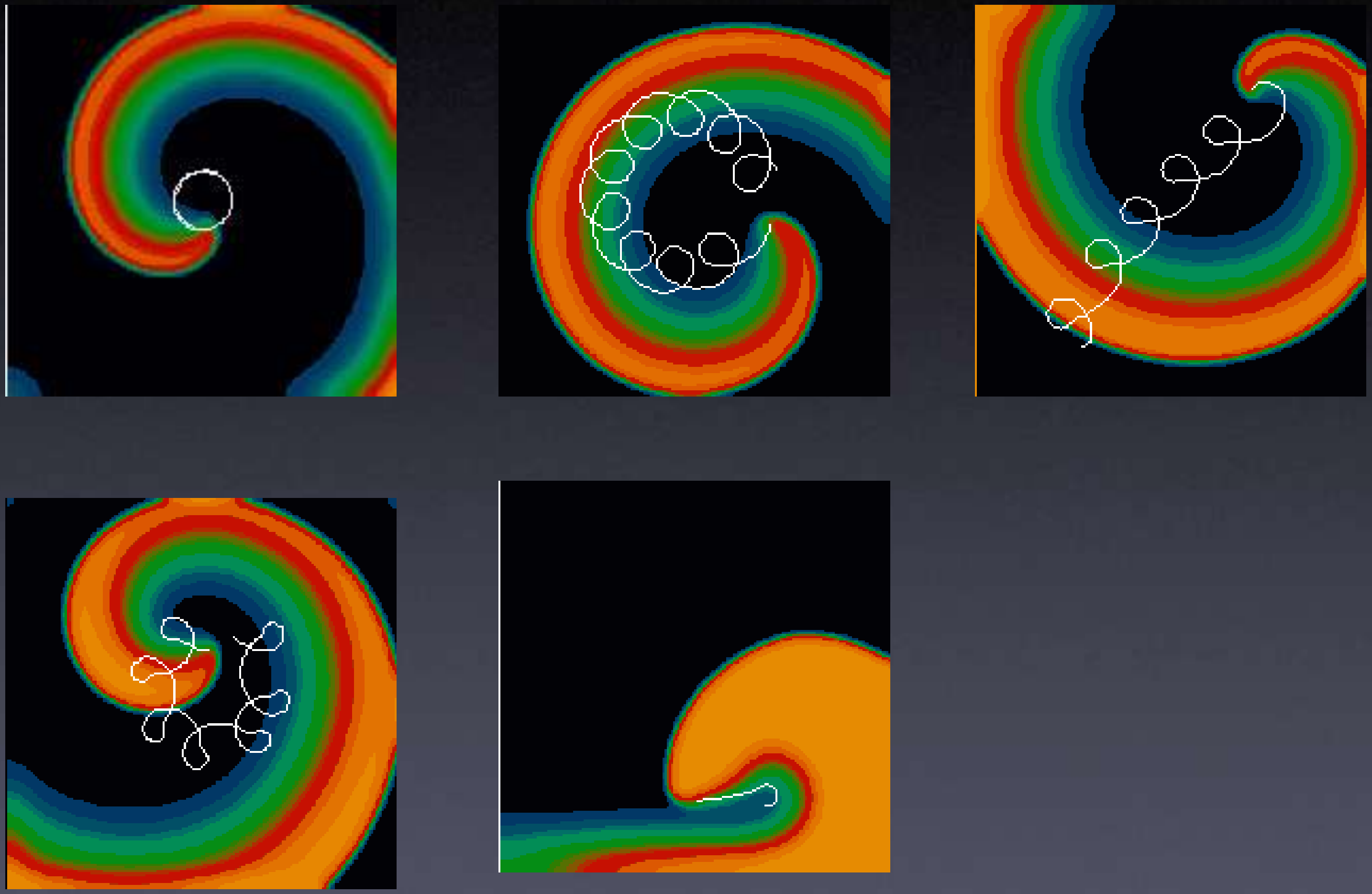

Fenton FH et al. Chaos 2002; 12, 852-892.

Reentrant Spiral Waves: Simulation

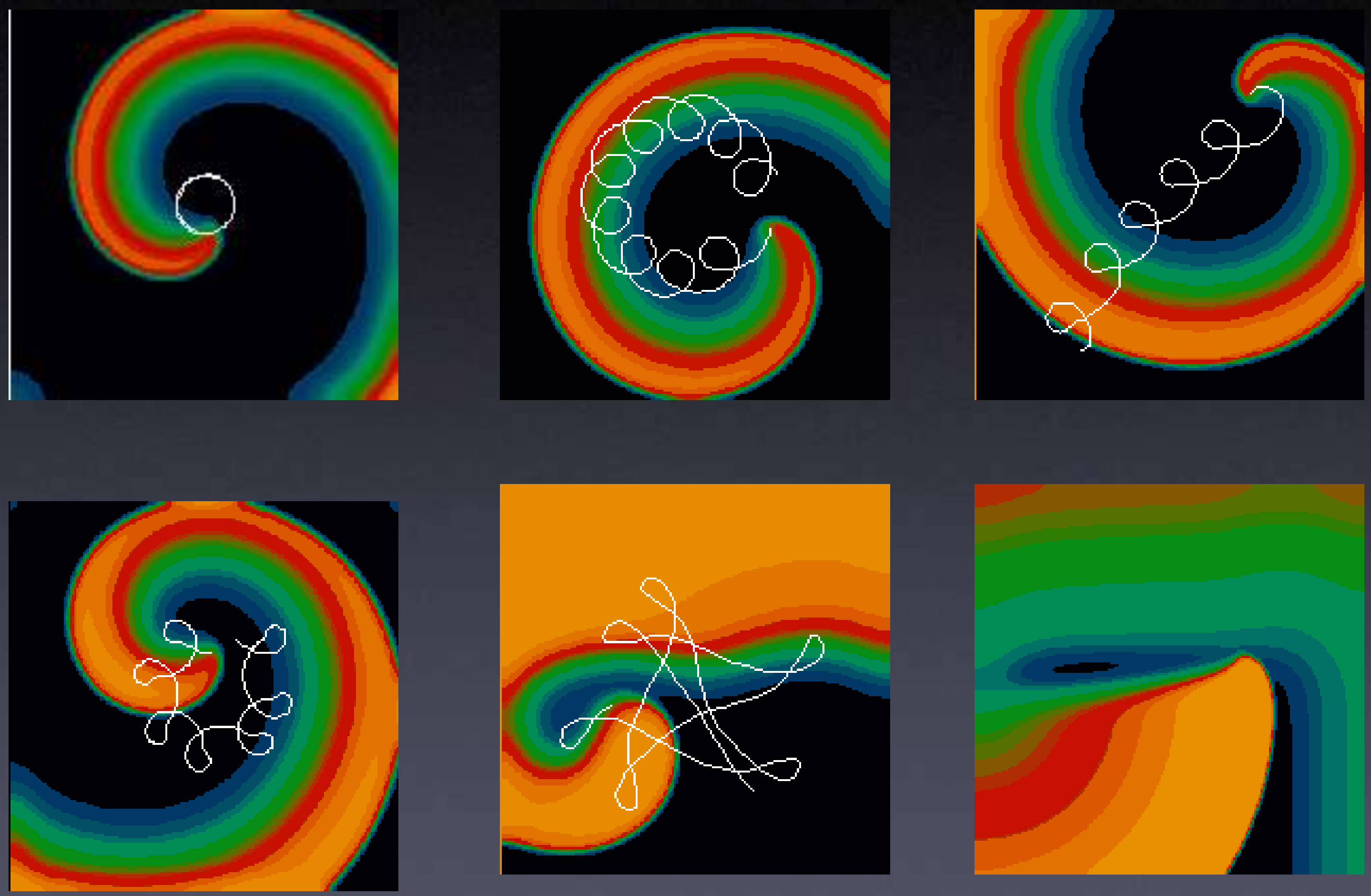

Fenton FH et al. Chaos 2002; 12, 852-892.

Reentrant Spiral Waves: Simulation

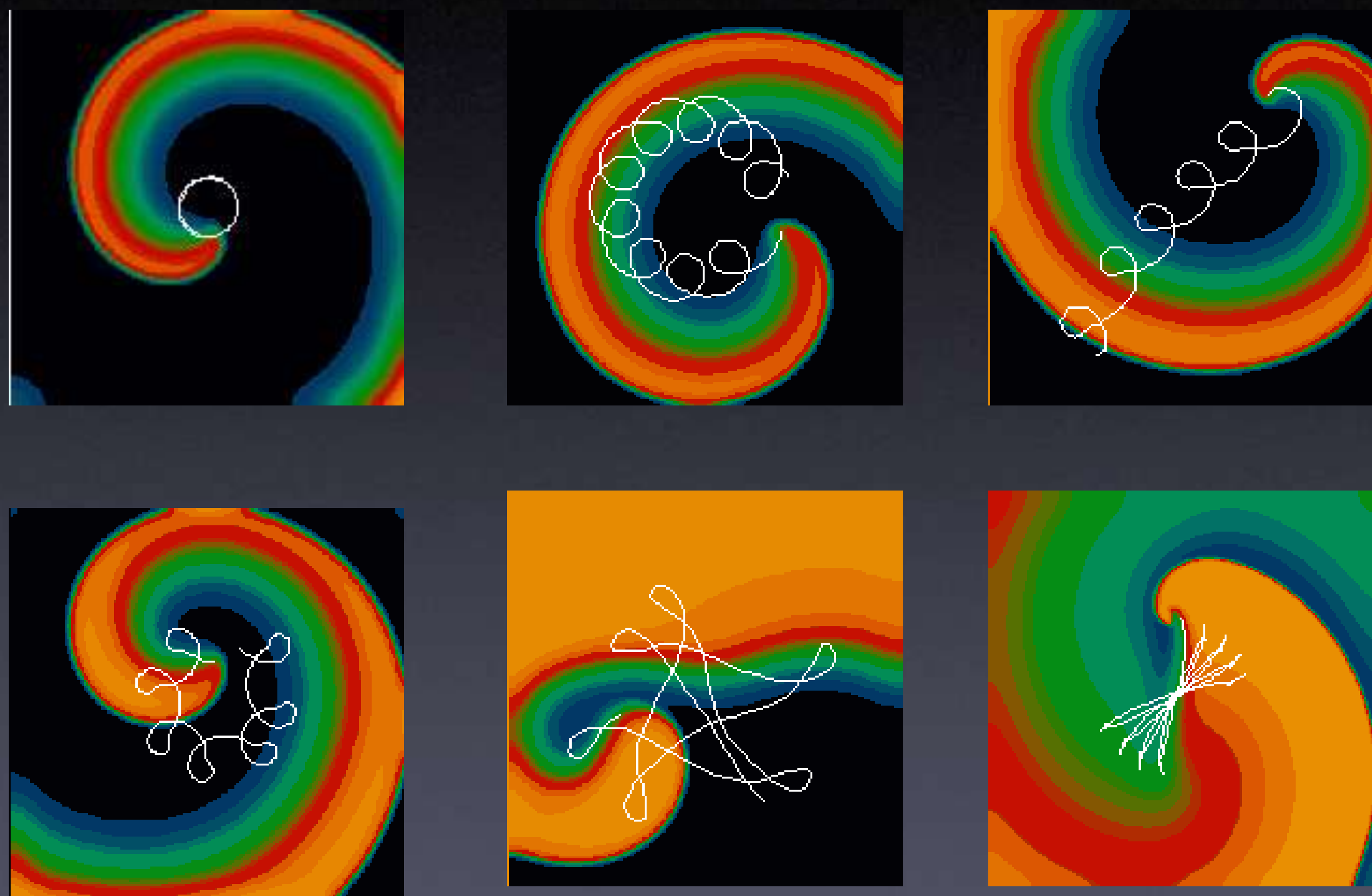

Fenton FH et al. Chaos 2002; 12, 852-892.

Spiral Waves: Experiment

Experimental spiral waves

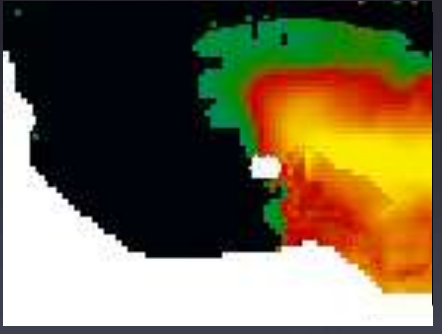

Circular core
Spiral wave

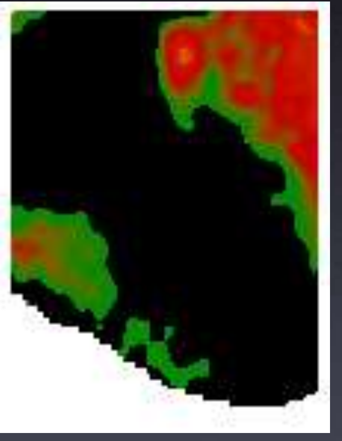

Linear core
Spiral wave

Cherry EM, Fenton FH. New Journal of Physics 2008; 10: 125016

How to Visualize Reentry in 3D?

2D → 3D

Spiral waves → Scroll waves

spiral tip vortex filament

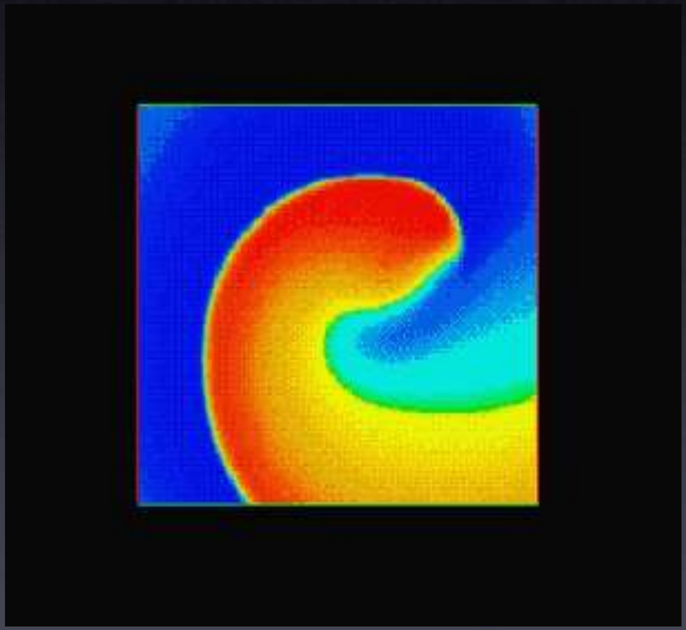

How to Visualize Reentry in 3D?

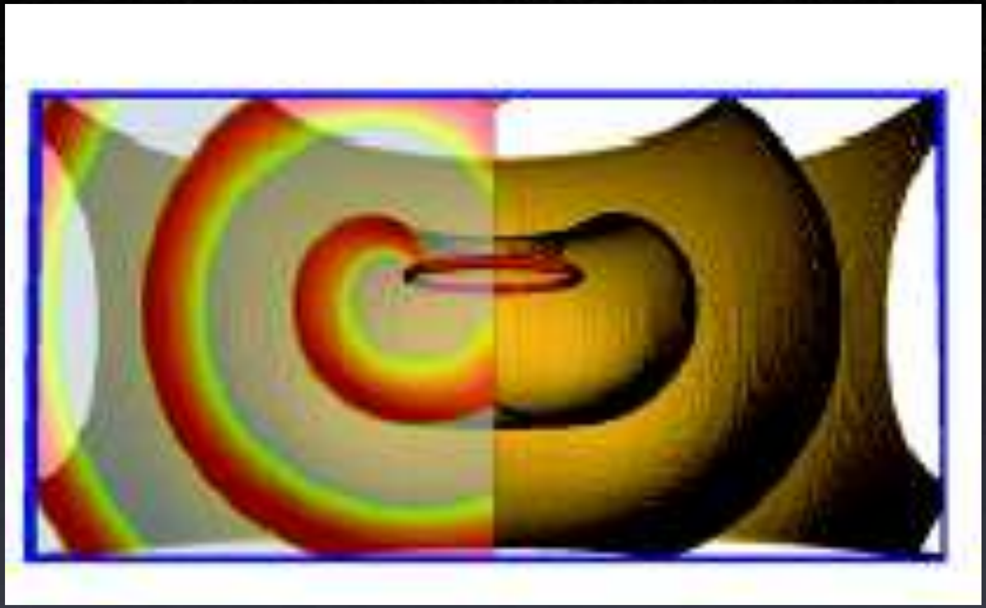

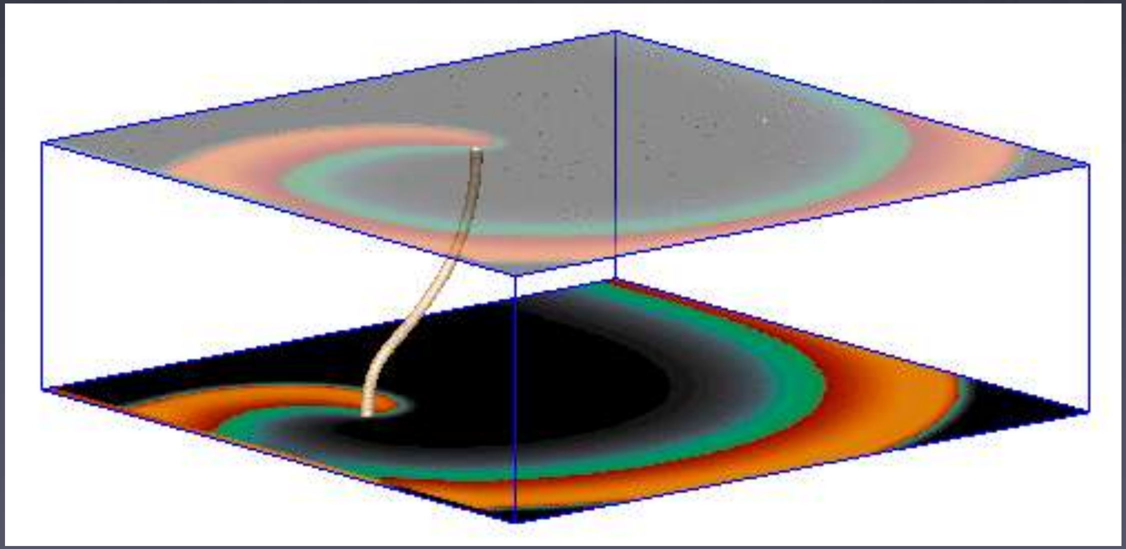

Similar to water spouts

How to Visualize Reentry in 3D?

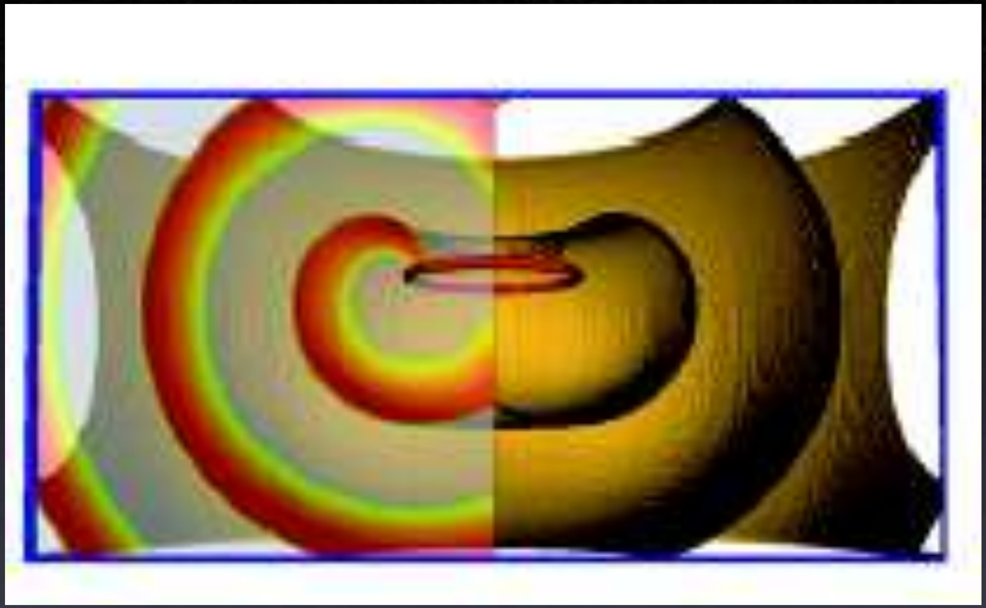

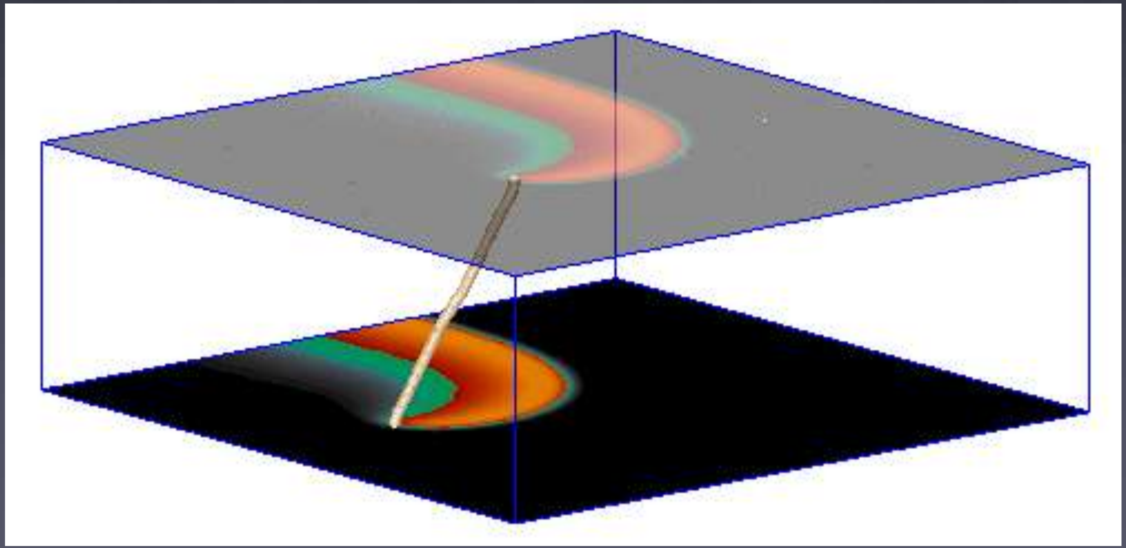

Vortex interactions

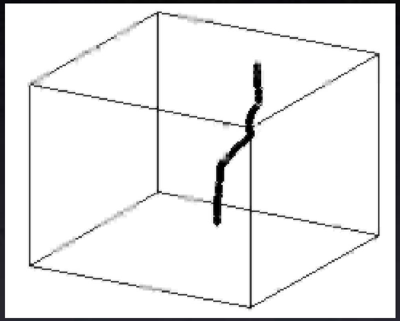

Ring creation

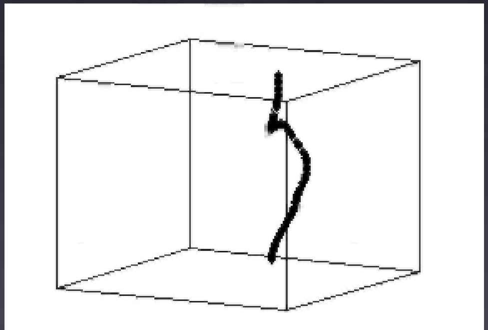

Ring fusion

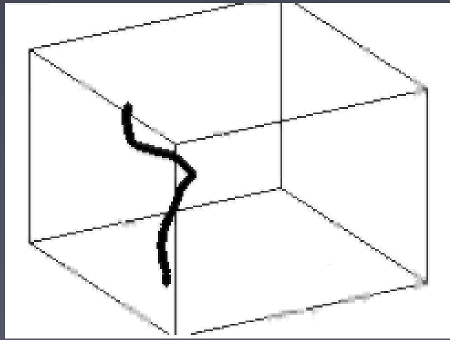

Vortex pinching

Many Models for Different Cell Types

Implemented most (~40) of the published models in single cells and in tissue.

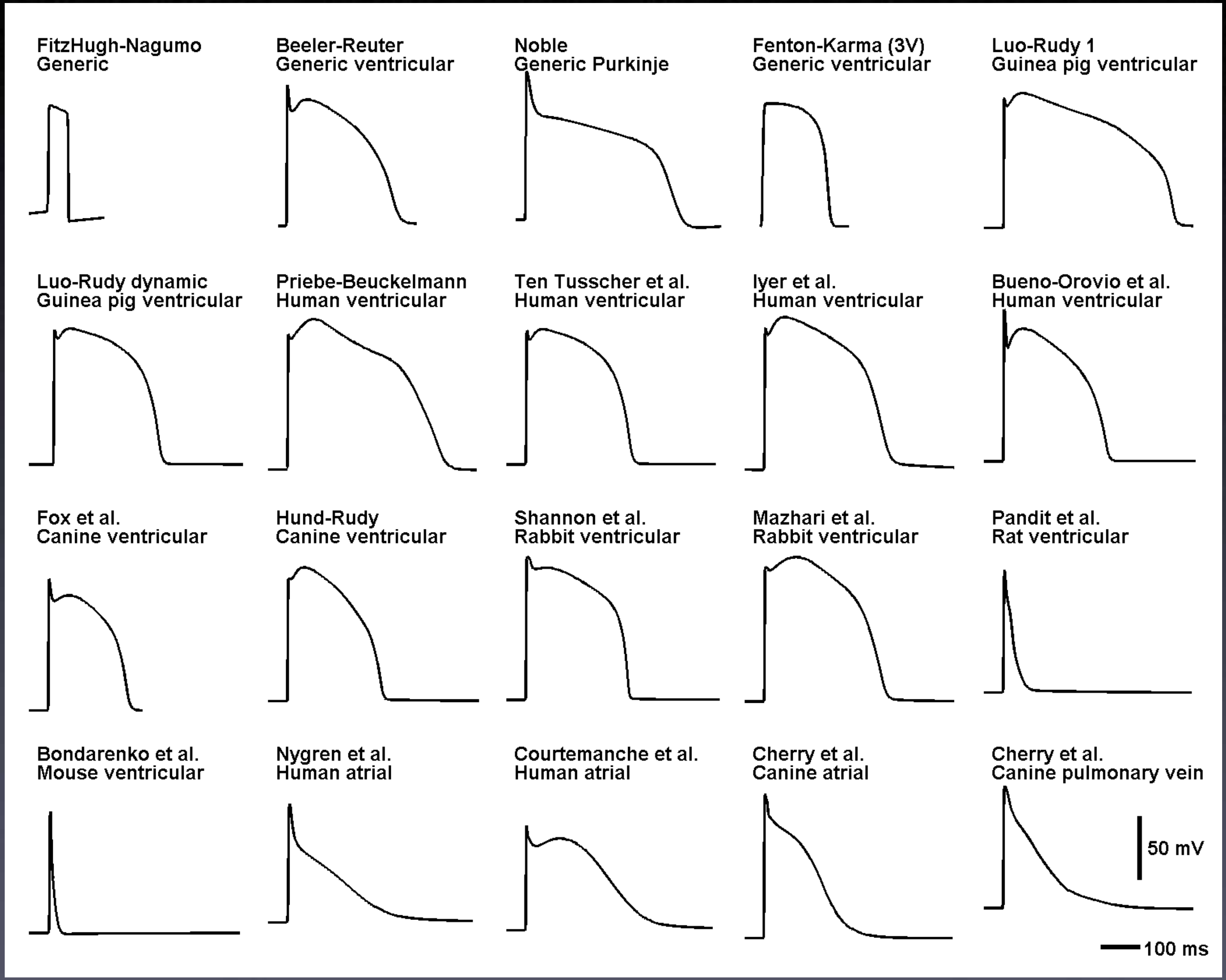

Fenton FH, Cherry EM, 2008. Models of cardiac cell. Scholarpedia 3, 1868.

Many Models for Different Cell Types

Implemented most (~40) of the published models in single cells and in tissue.

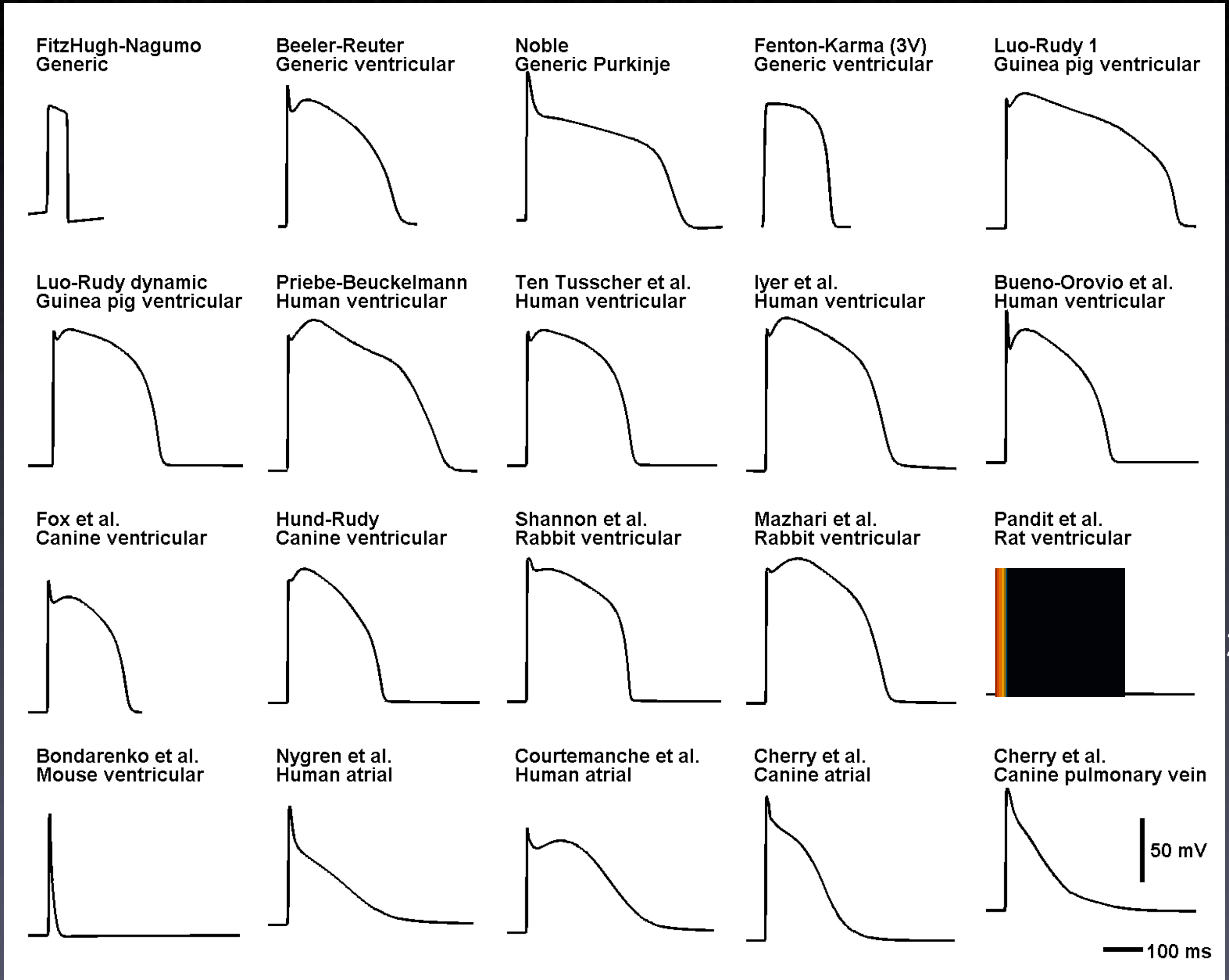

26 variables
2D (200x200x26
=1,040,000)

dt ~ .01ms
1s of simulation =
1,040,000*100000
$=1x10^{11}$

Fenton FH, Cherry EM, 2008. Models of cardiac cell. Scholarpedia 3, 1868.

Many Models for Different Cell Types

Implemented most (~40) of the published models in single cells and in tissue.

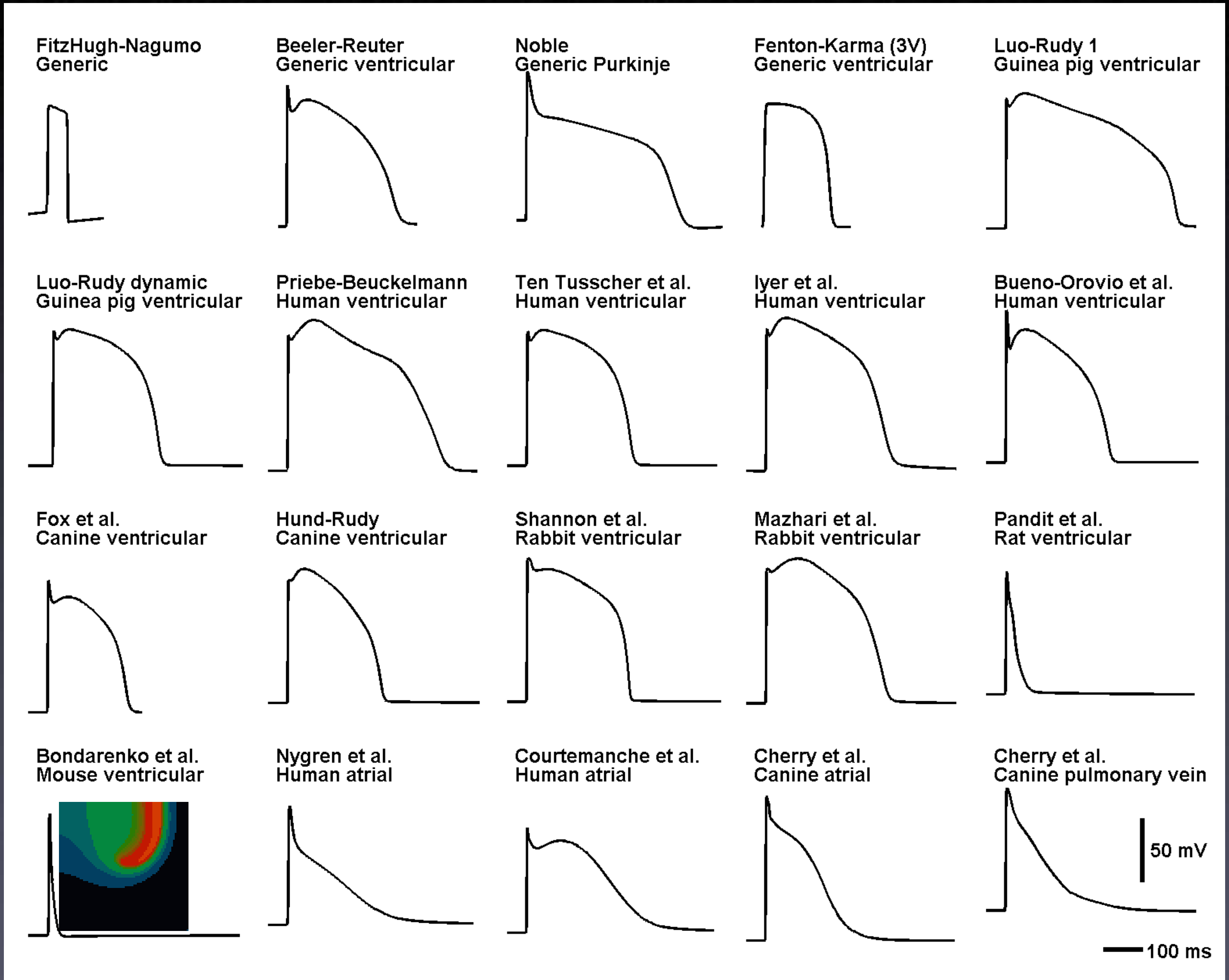

Fenton FH, Cherry EM, 2008. Models of cardiac cell. Scholarpedia 3, 1868.

Many Models for Different Cell Types

Implemented most (~40) of the published models in single cells and in tissue.

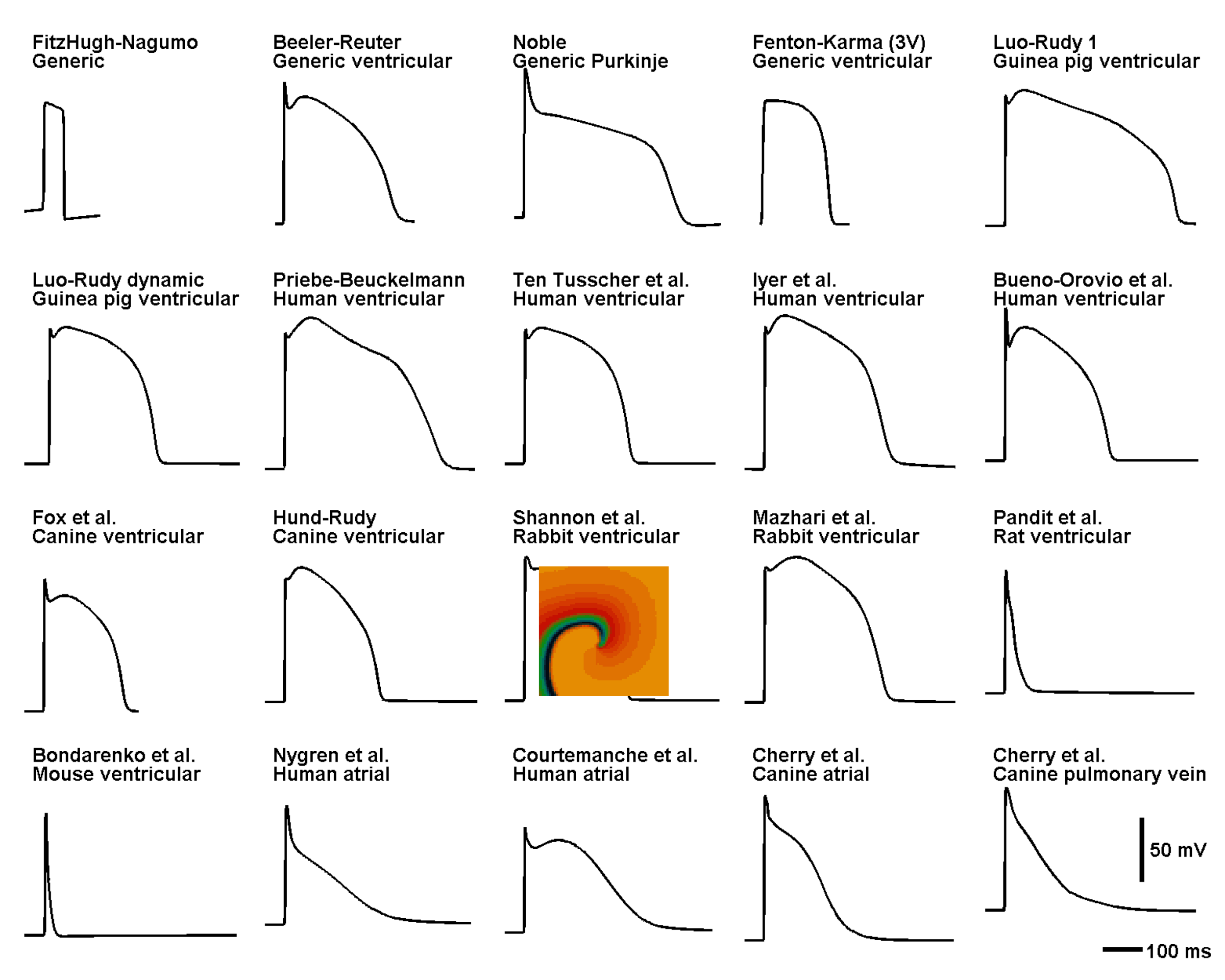

Fenton FH, Cherry EM, 2008. Models of cardiac cell. Scholarpedia 3, 1868.

Many Models for Different Cell Types

Implemented most (~40) of the published models in single cells and in tissue.

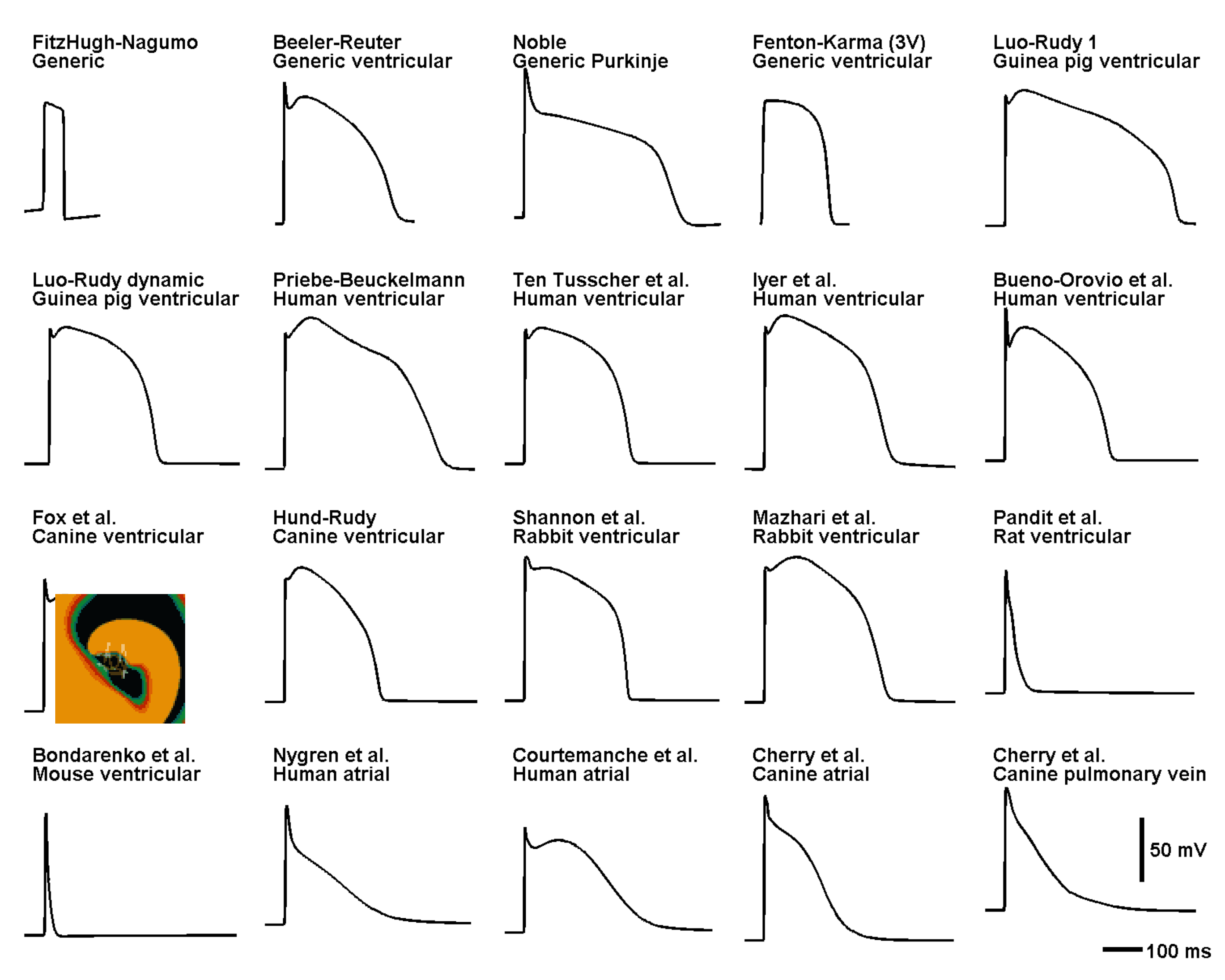

Fenton FH, Cherry EM, 2008. Models of cardiac cell. Scholarpedia 3, 1868.

Many Models for Different Cell Types

Implemented most (~40) of the published models in single cells and in tissue.

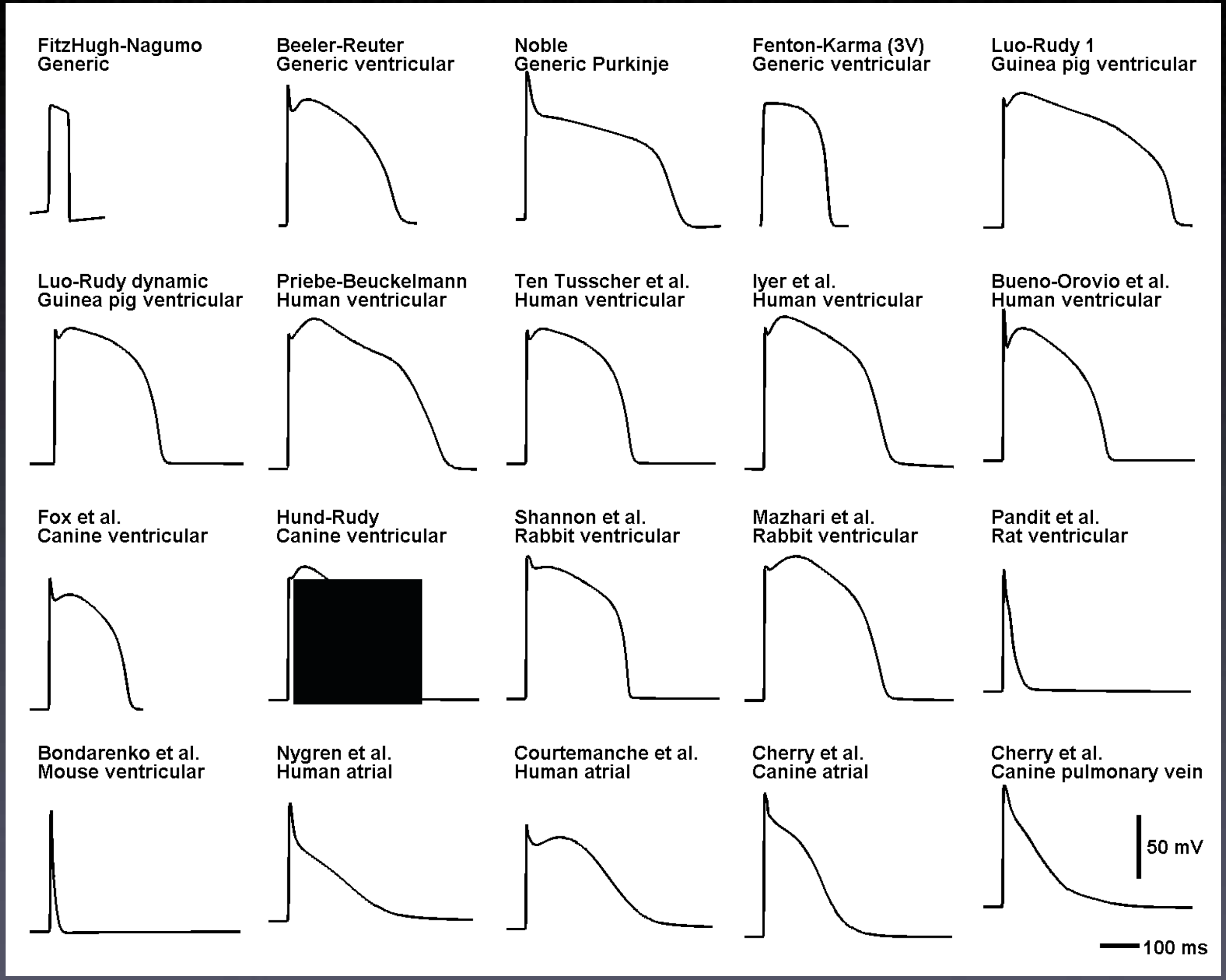

Fenton FH, Cherry EM, 2008. Models of cardiac cell. Scholarpedia 3, 1868.

Many Models for Different Cell Types

Implemented most (~40) of the published models in single cells and in tissue.

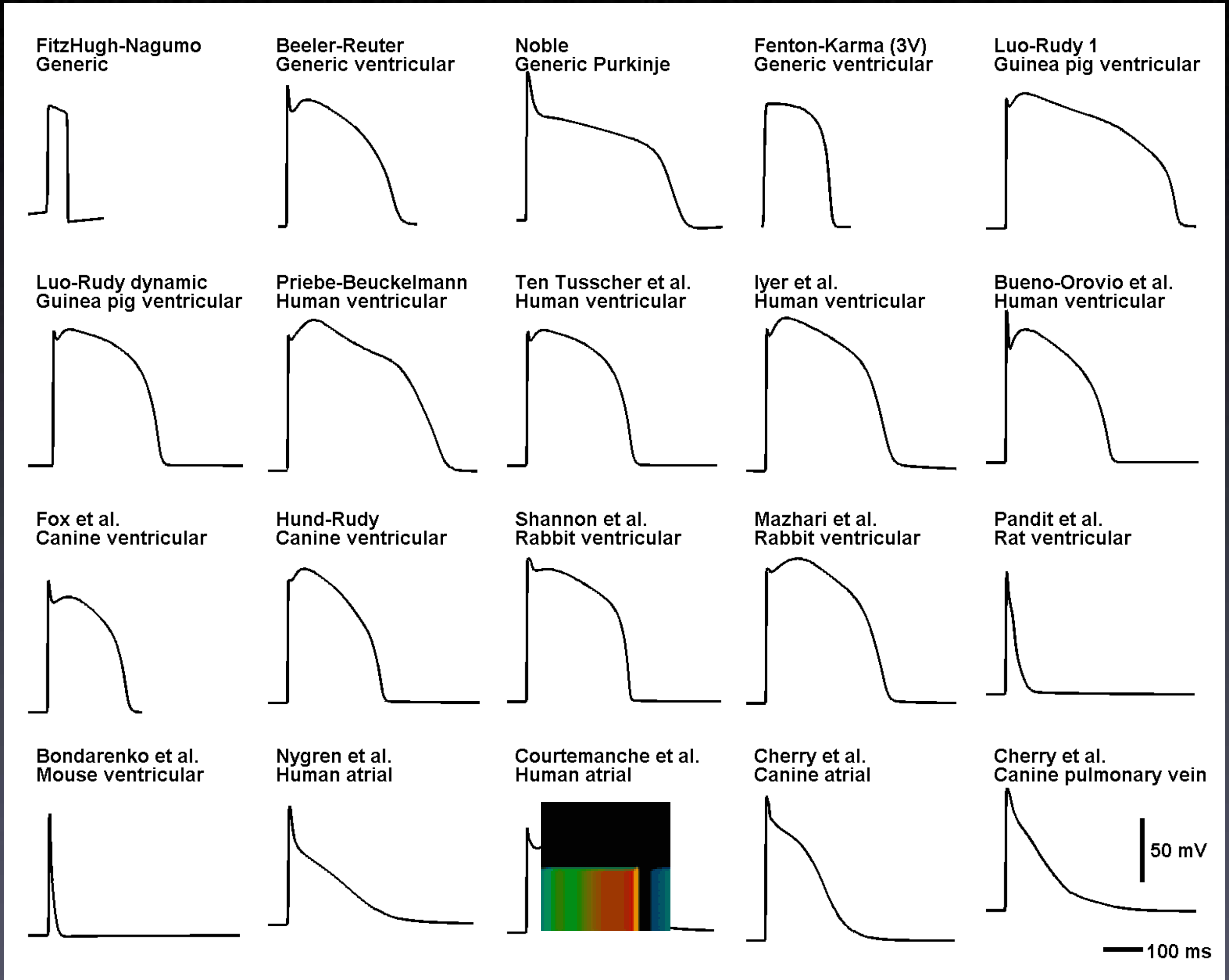

Fenton FH, Cherry EM, 2008. Models of cardiac cell. Scholarpedia 3, 1868.

Many Models for Different Cell Types

Implemented most (~40) of the published models in single cells and in tissue.

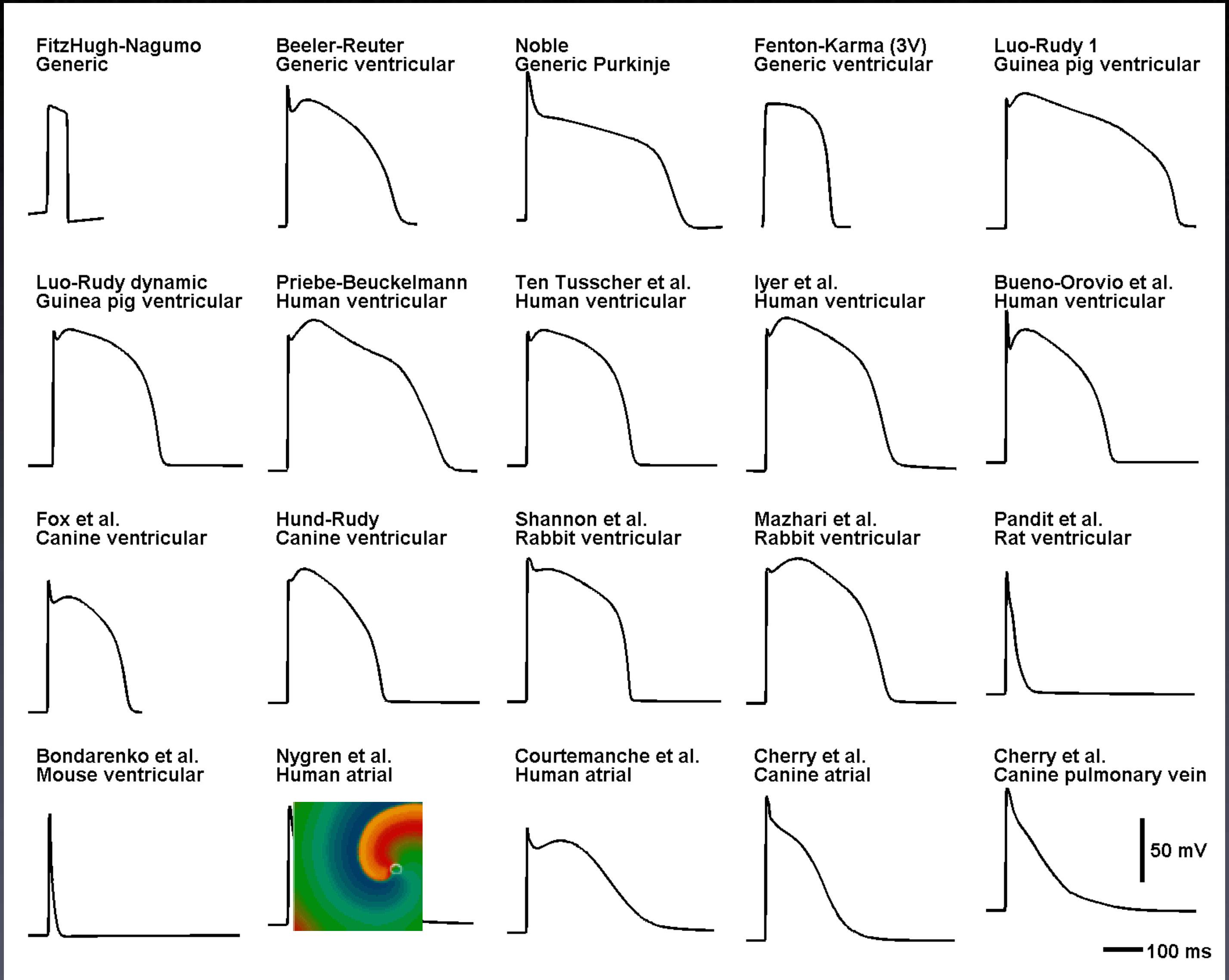

Fenton FH, Cherry EM, 2008. Models of cardiac cell. Scholarpedia 3, 1868.

Many Models for Different Cell Types

Implemented most (~40) of the published models in single cells and in tissue.

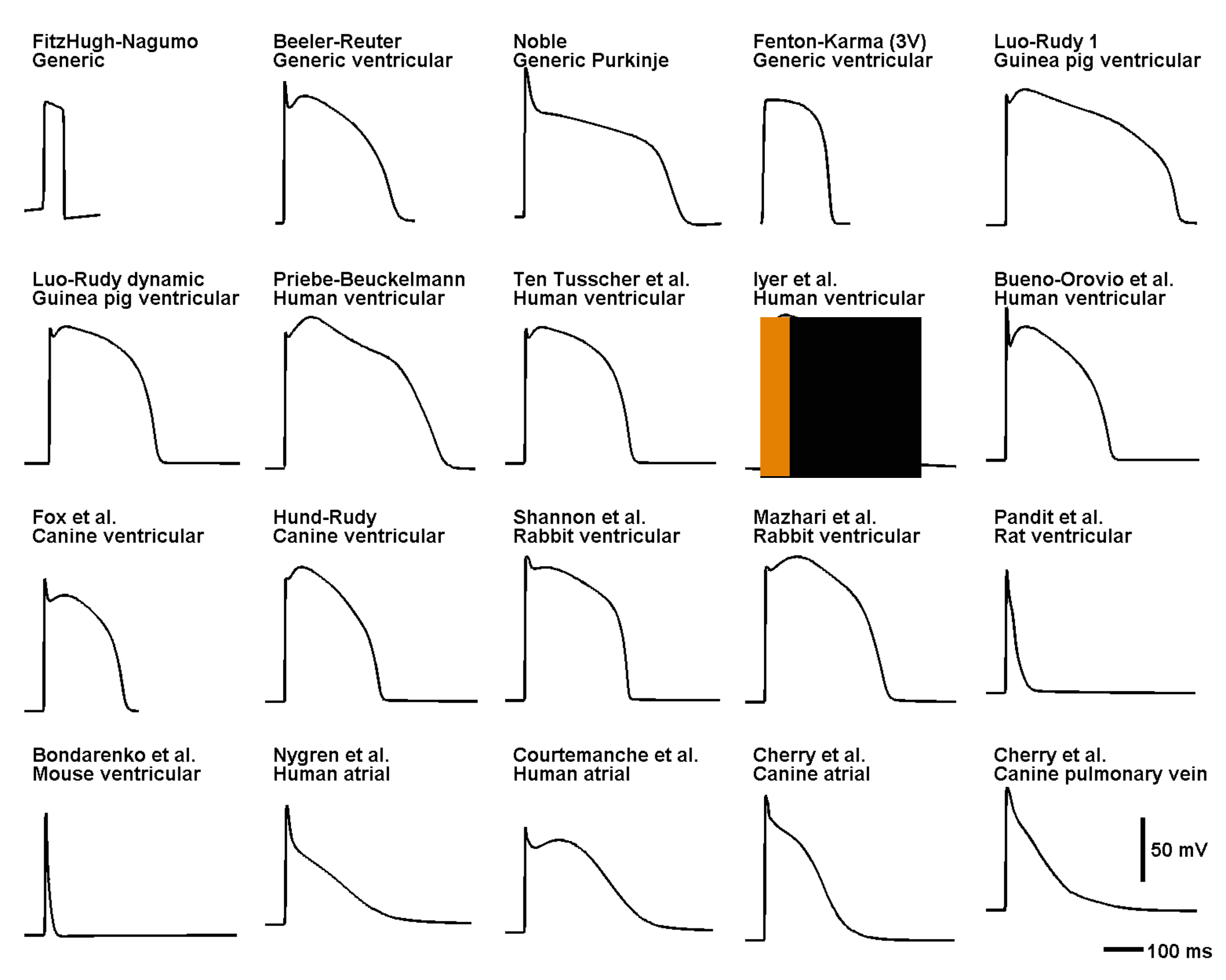

67 variables
2D (200x200x67
=2,680,000)

Fenton FH, Cherry EM, 2008. Models of cardiac cell. Scholarpedia 3, 1868.

Many Models for Different Cell Types

Implemented most (~40) of the published models in single cells and in tissue.

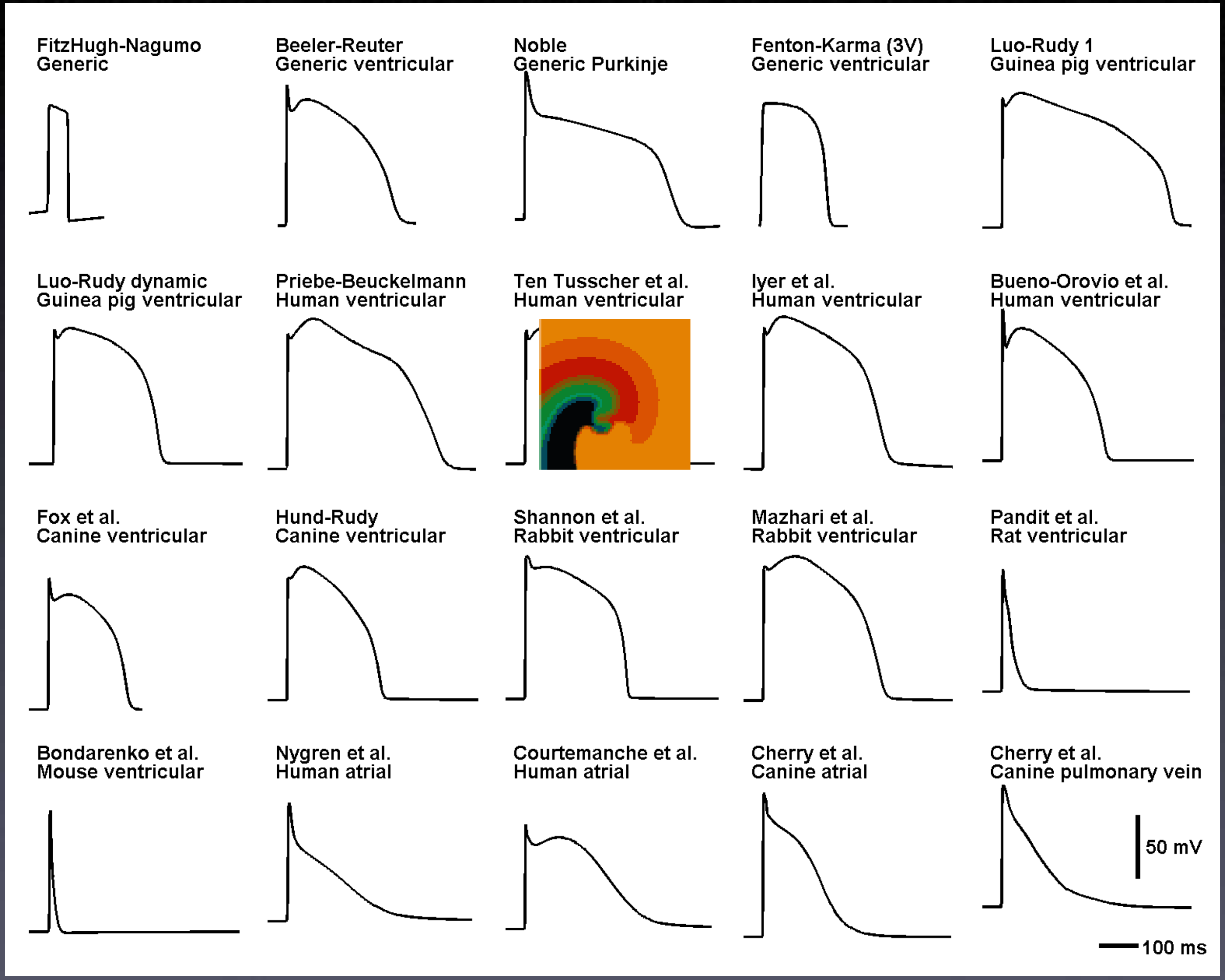

Fenton FH, Cherry EM, 2008. Models of cardiac cell. Scholarpedia 3, 1868.

Many Models for Different Cell Types

Implemented most (~40) of the published models in single cells and in tissue.

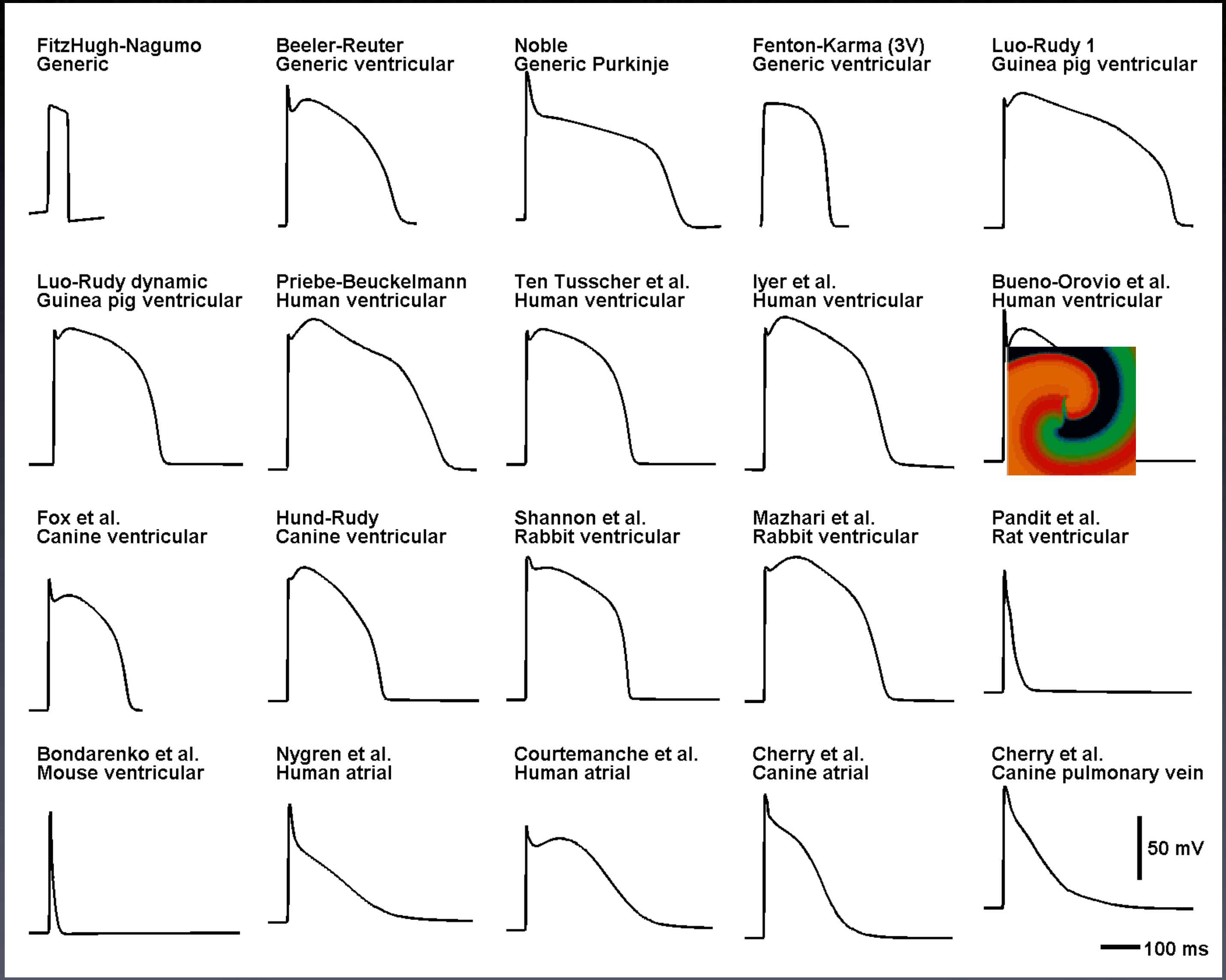

Fenton FH, Cherry EM, 2008. Models of cardiac cell. Scholarpedia 3, 1868.

Anatomically Realistic Model of Human Atria

Dimensions:

7.5cm x 7cm x 5.5cm

2.5 million nodes

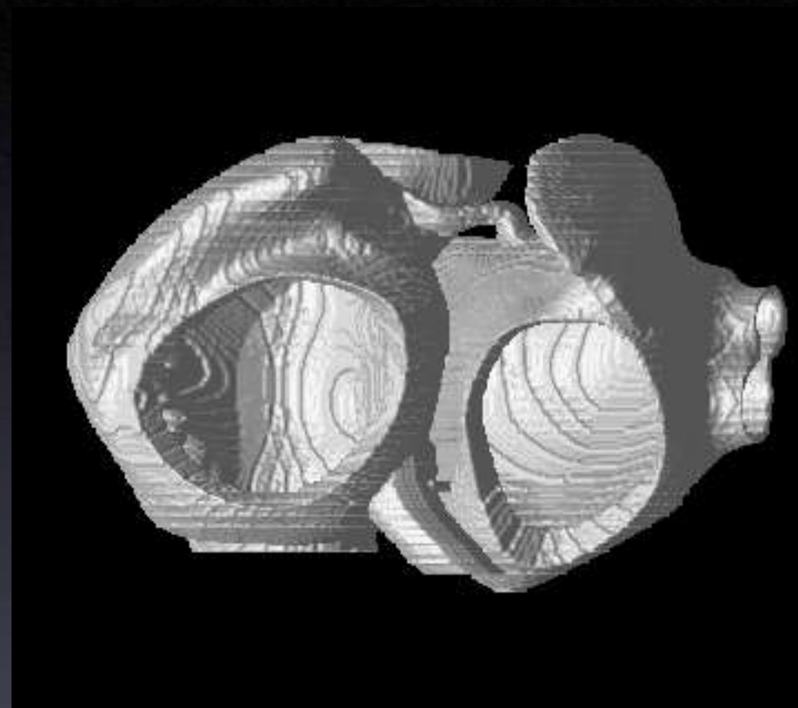

Harrild and Henriquez, 2000
+ coronary sinus

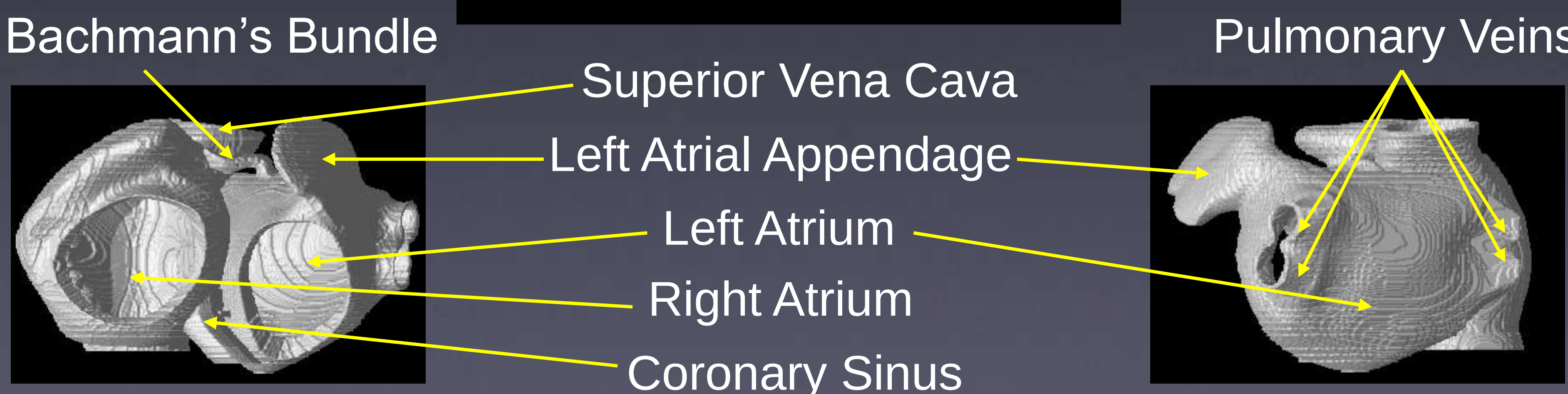

Bundle Conductivities

Healthy atria

Fast CV: 150 cm/

Bulk CV: 60 cm/s

Slow CV: 35 cm/s

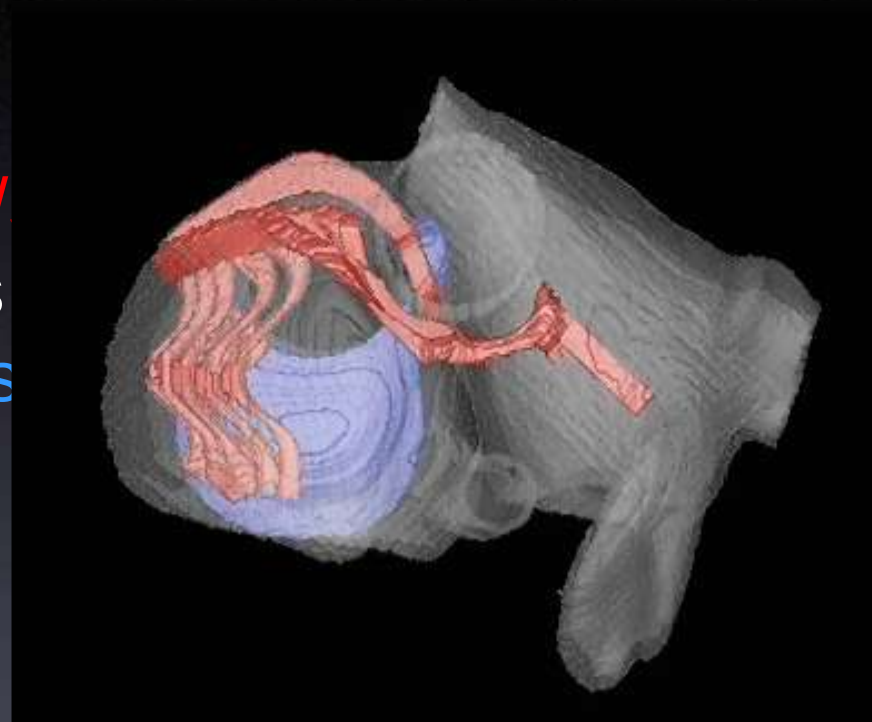

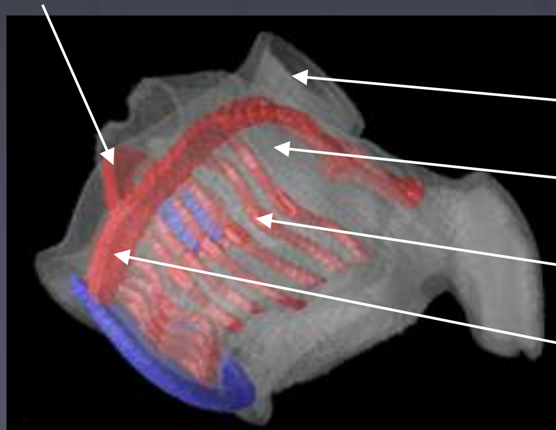

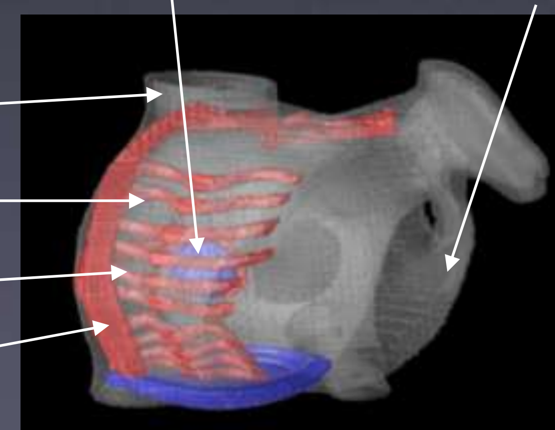

Example of Simulated AT and AF

Reentry in the Atrial Model

Atrial Tachycardia

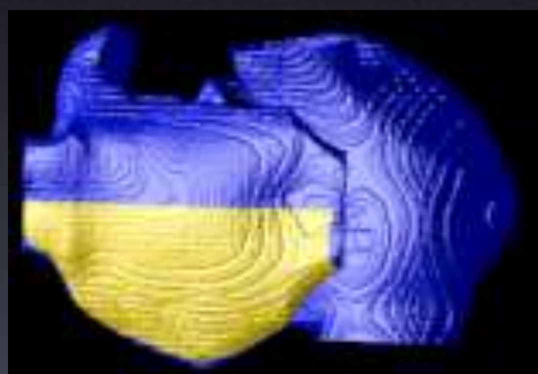

Atrial Fibrillation

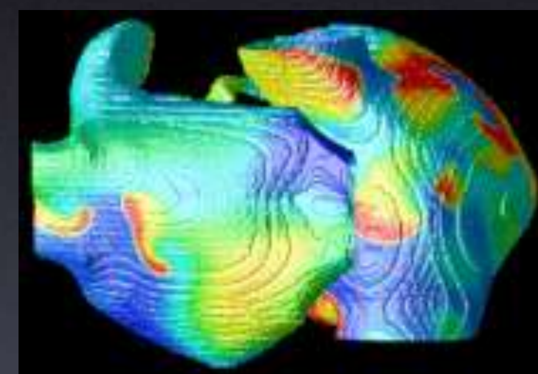

How to terminate reentrant arrhythmias?

Modeling AF Ablation

Left atrial lines only

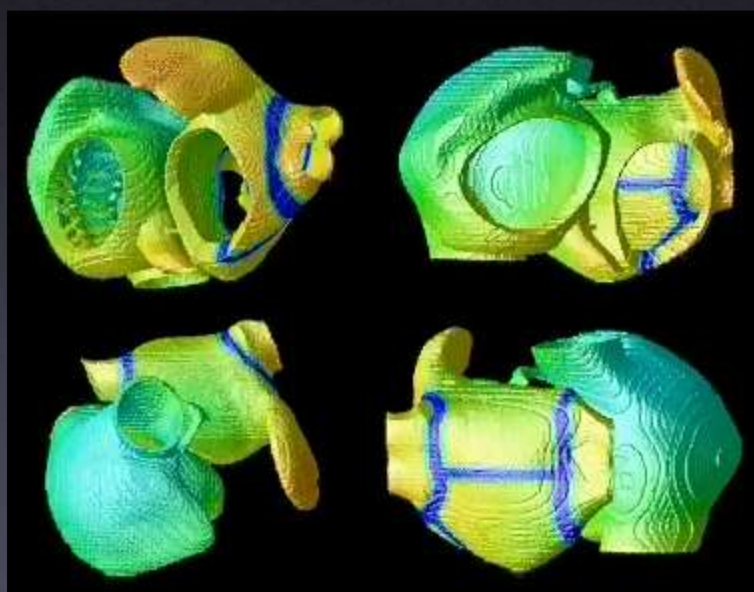

Left + right lines

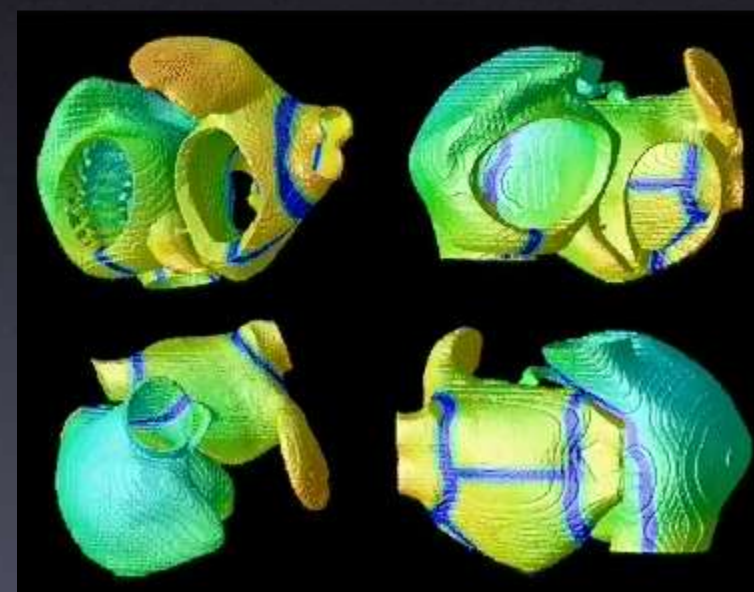

Modeling AF defibrillation

- Electrical therapies
  - ATP (effective only for slow tachycardias)
  - Electrical cardioversion (requires >5V/cm)[1]

    External ~ 100J - 280J up to 360J (1000V, 30-45 A)[3]

    Internal ~7J (350V, 4 A)[2]

1 Ideker RE, Zhou X, Knisley SB.
Pacing Clin Electrophysiol 1995;18:512-525.
2 Santini et al. J Interv Card Electrophysiol 1999;3:45-51.
3 Koster et al. Am Heart J 2004;147:e20-e26.

New method for defibrillation

- Demonstrate that cardioversion can be achieved by a series of far-field low-energy pulses (~1.4V/cm) delivered at a frequency close to the dominant frequency of the arrhythmia.
- Internal ~7J (350V, 4 A) → (requires >5V/cm)
- This method is based on the idea of recruitment of virtual electrodes in cardiac tissue and global synchronization.

Virtual electrodes and secondary sources

Example with large holes was a proof of concept

Not only large holes but also smaller conductivity discontinuities can act as "virtual electrodes."

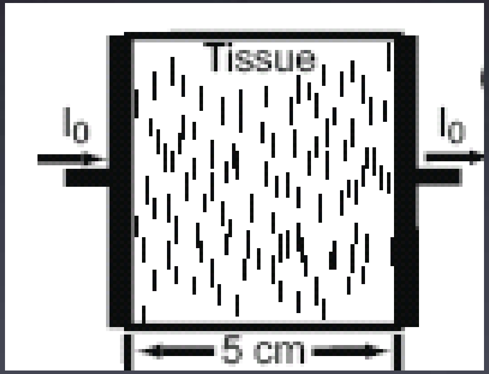

Virtual electrodes and secondary sources

Example with large holes was a proof of concept

Not only large holes but also smaller conductivity discontinuities can act as "virtual electrodes."

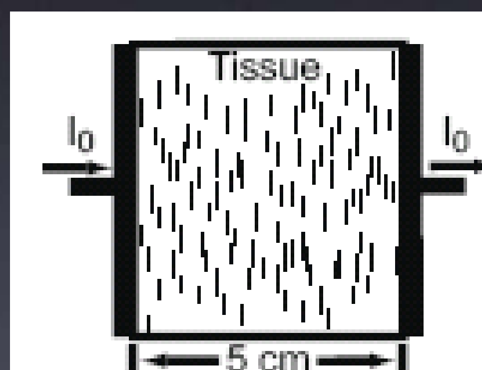

Field Strength
E = 0.6 V/cm

Field Strength
E = 1.2 V/cm

Bidomain (GMRES)
dx=.01 cm, dt=.01ms
Zero flux B.C.s, finite volume
I_{ion}: Fox et al. model
Collagen ~.065cm

Virtual electrodes and secondary sources

Example with large holes was a proof of concept

Not only large holes but also smaller conductivity discontinuities can act as "virtual electrodes."

The more "virtual electrodes" recruited, the faster the whole tissue is excited.

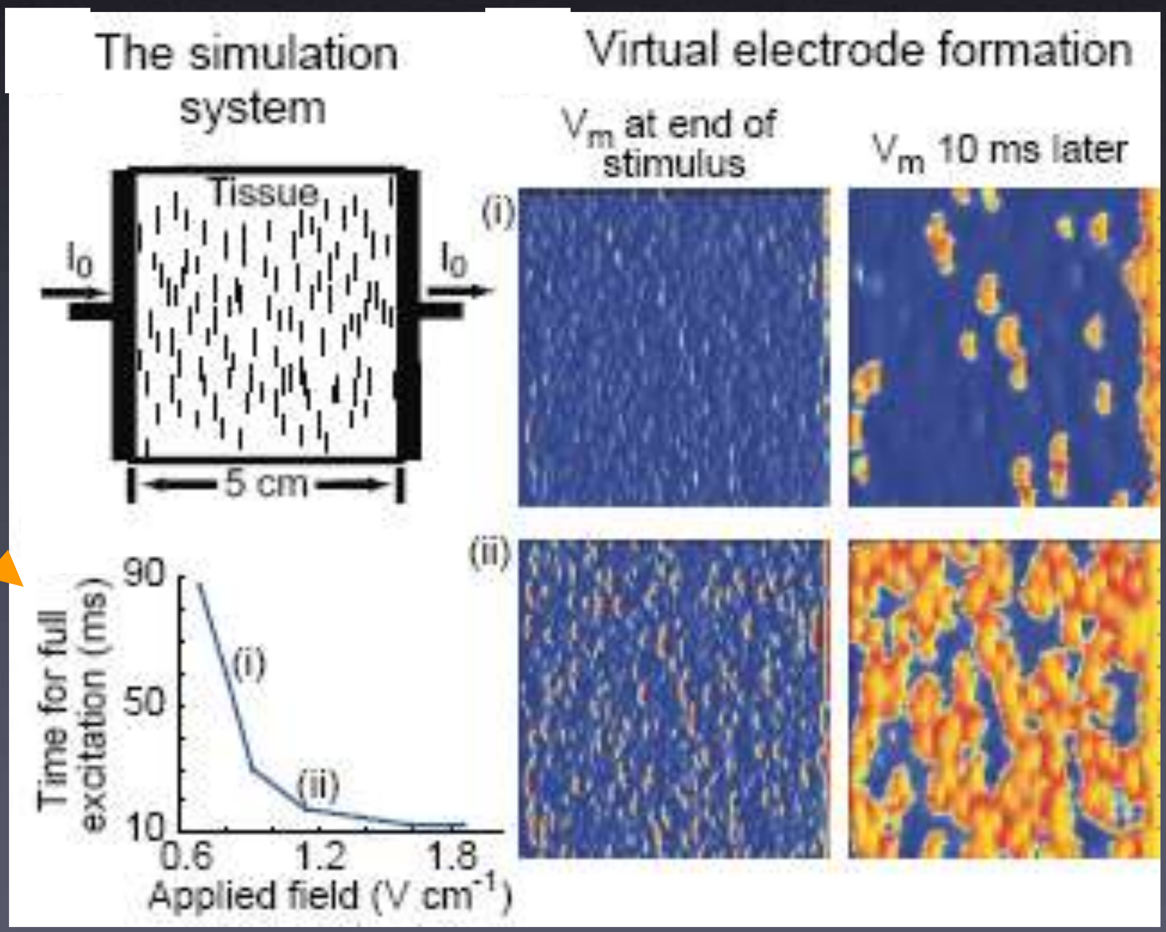

Defibrillation via Virtual Electrodes by synchronization

Termination of spiral waves in simulated cardiac tissue by 4 low-energy shocks.

Bidomain (GMRES)
dx=.01cm, dt=.01ms
Zero flux B.C.s, finite volume
I_{ion}: Nygren et al. atrial cell model
Collagen ~.065cm

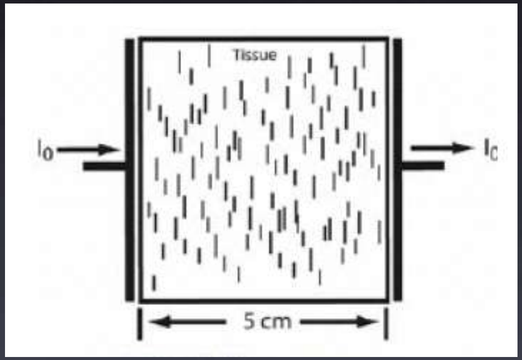

As the tissue synchronizes to the pacing period, more tissue gets activated simultaneously, and the reentries are terminated.

Defibrillation via Virtual Electrodes by synchronization

Termination of spiral waves in simulated cardiac tissue by 4 low-energy shocks.

Bidomain (GMRES)
dx=.01cm, dt=.01ms
Zero flux B.C.s, finite volume
I_{ion}: Nygren et al. atrial cell model
Collagen ~.065cm

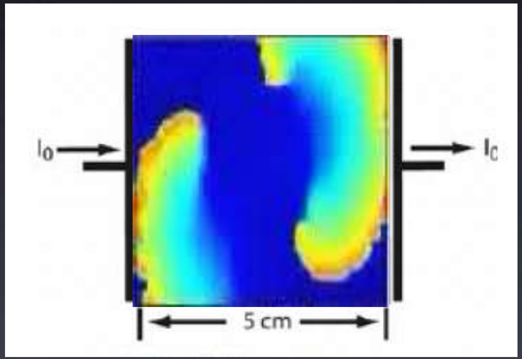

As the tissue synchronizes to the pacing period, more tissue gets activated simultaneously, and the reentries are terminated.

Defibrillation via Virtual Electrodes by synchronization

Termination of spiral waves in simulated cardiac tissue by 4 low-energy shocks.

Bidomain (GMRES)
dx=.01cm, dt=.01ms
Zero flux B.C.s, finite volume
I_{ion}: Nygren et al. atrial cell model
Collagen ~.065cm

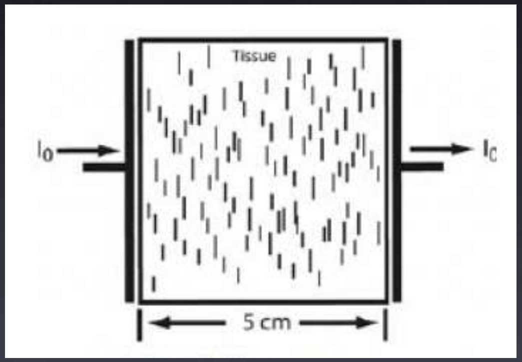

FTE

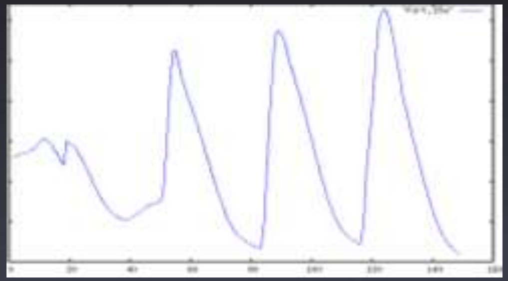

FTE/dt

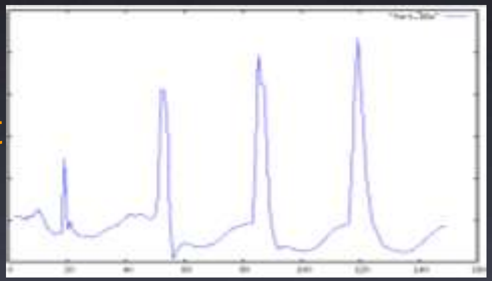

As the tissue synchronizes to the pacing period, more tissue gets activated simultaneously, and the reentries are terminated.

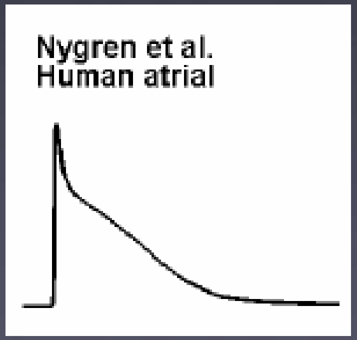

Examples of low-energy far-field stimulation

Examples of low-energy far-field stimulation

- Cardioversion success

E=1.4 V/cm

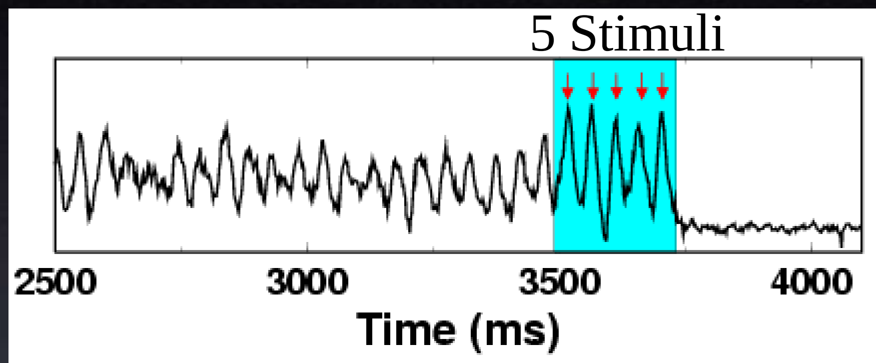

Fenton et al., Circulation 2009;120:467-476

Examples of low-energy far-field stimulation

- Cardioversion success

E=1.4 V/cm

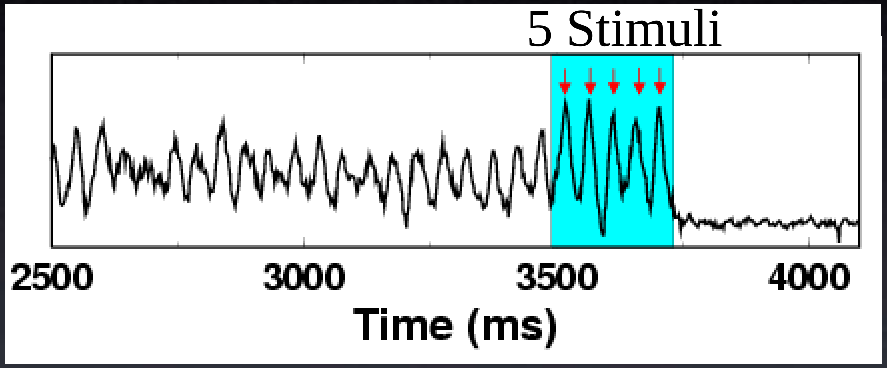

Fenton et al., Circulation 2009;120:467-476

Examples of low-energy far-field stimulation

- Cardioversion success

E=1.4 V/cm

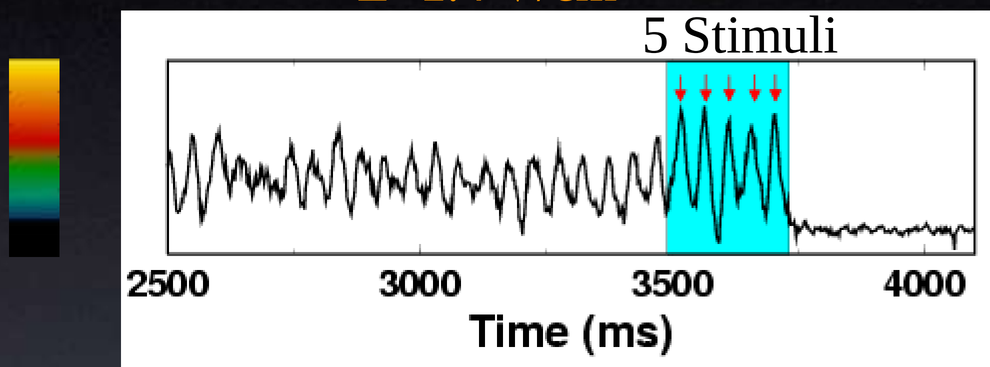

- Cardioversion failure

E=0.93 V/cm

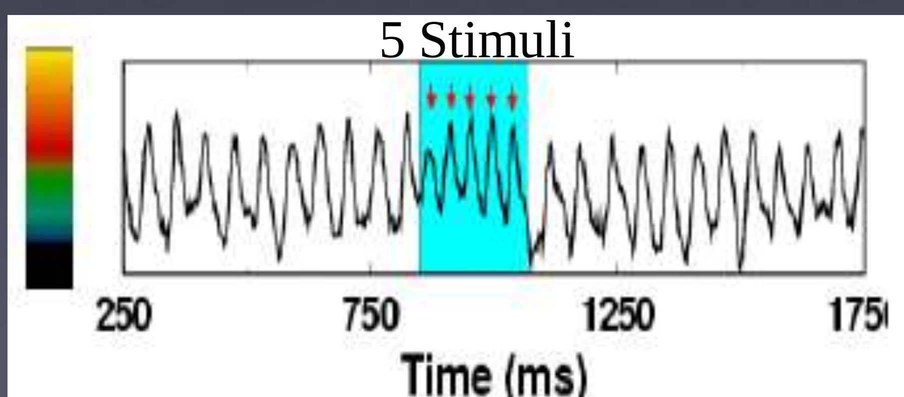

Fenton et al., Circulation 2009;120:467-476

Examples of low-energy far-field stimulation

- Cardioversion success

E=1.4 V/cm

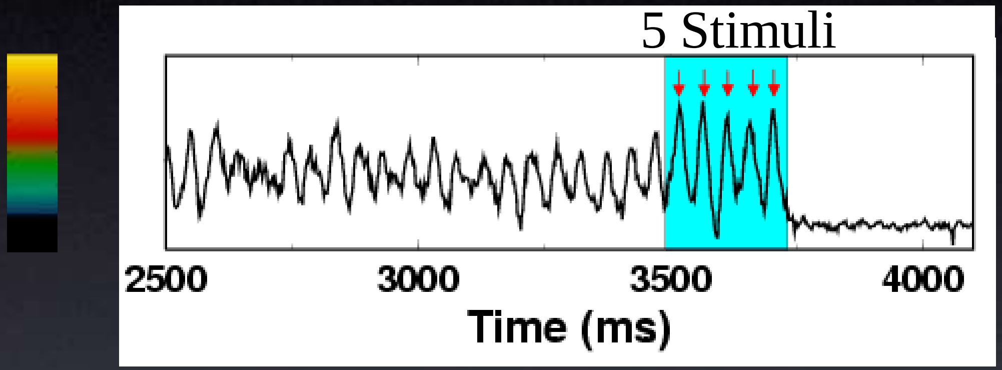

- Cardioversion failure

E=0.93 V/cm

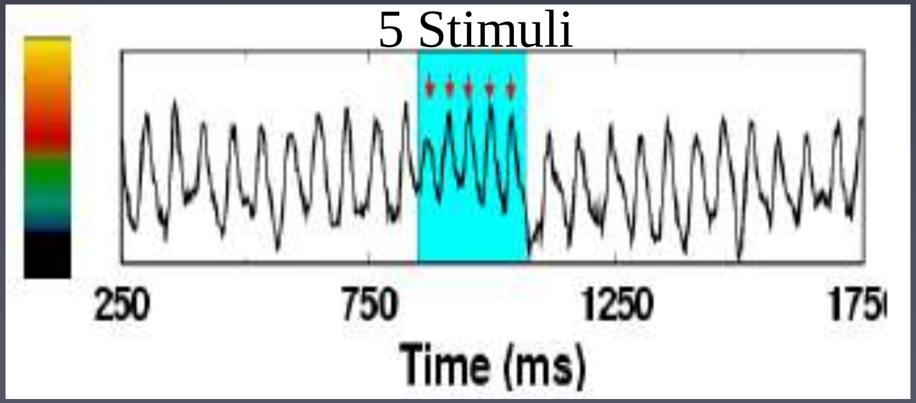

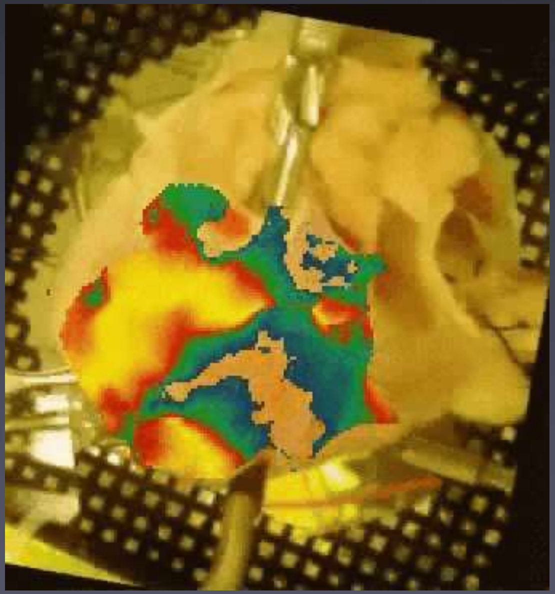

Fenton et al., Circulation 2009;120:467-476

Examples of low-energy far-field stimulation and single high-enrgy pulse cardioversion

FF Failure E=0.9 V/cm

FF Success E=1.4 V/cm

Cardioversion Failure E=4.0 V/cm

Cardioversion Success E=4.67 V/cm

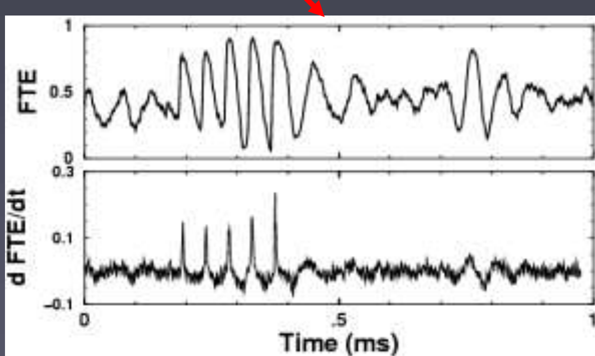

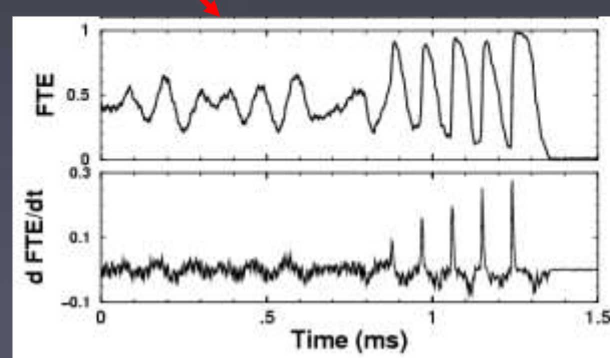

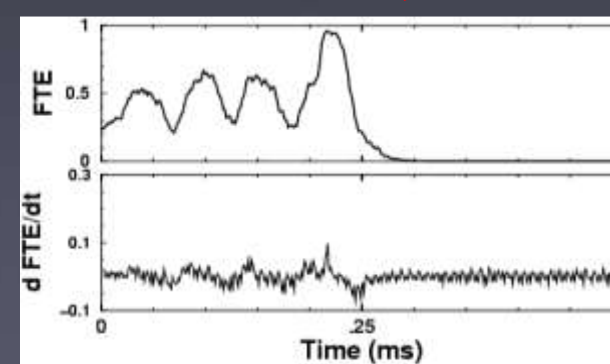

Examples of low-energy far-field stimulation in different preparations
Dominant periods 30 - 60 ms

Success rate of 93 percent (69/74 trials in 8 canine atrial preparations).

Successful defibrillation using FF-AFP ranged between 0.074 and 0.81 J, with an average of 0.24 J,

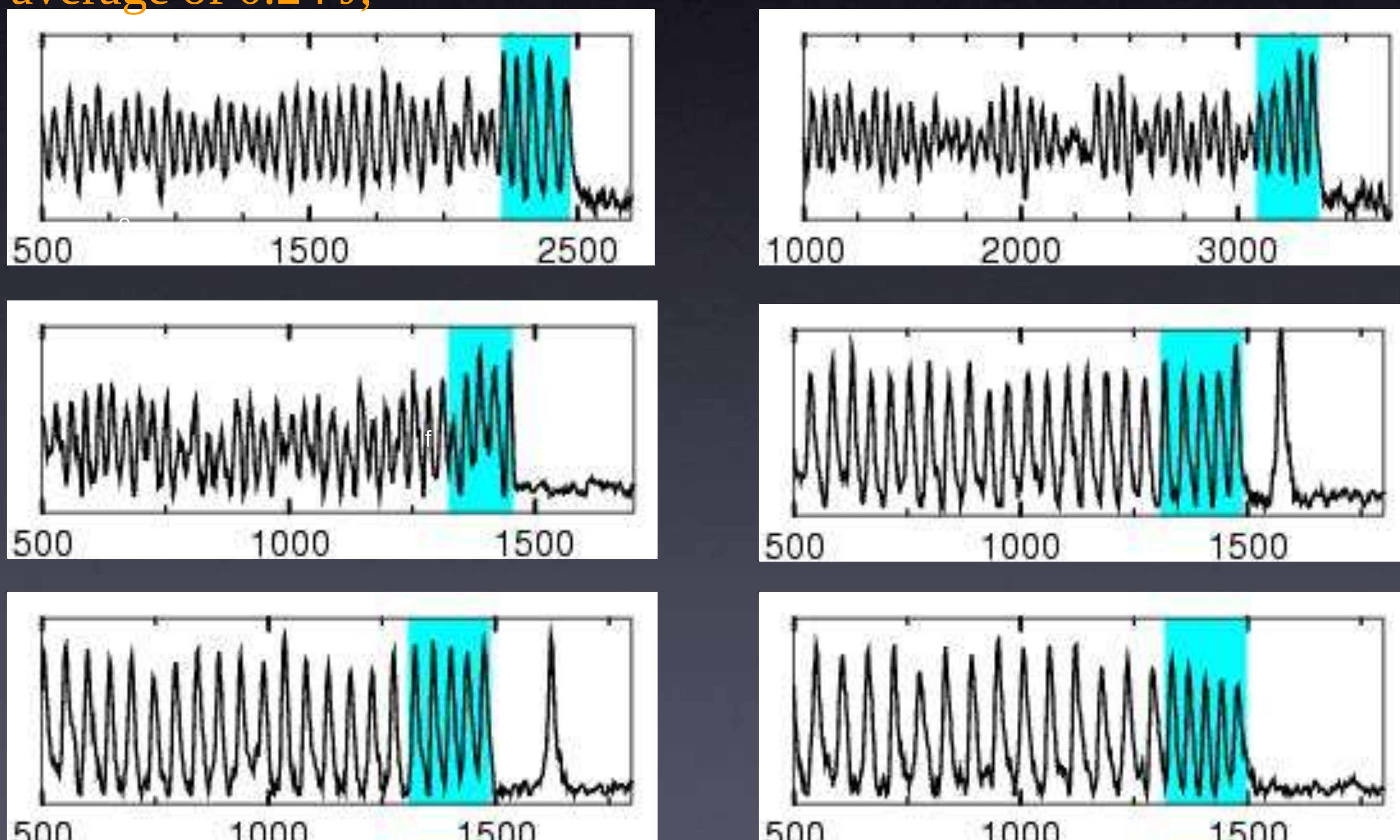

Fenton et al., Circulation 2009;120:467-476

Overview of Project

S Smolka, R Grosu, J. Glimm, R. Gilmour, F. Fenton

Year 1-2

- Model Checking and abstraction
- Atrial detail models ←→ Minimal models ←→ Hybrid automata models
- Experimental data (normal and disease)
- Characteristics with model checking

Specific Criteria:

Single cell:

- Threshold for excitation
- dV/dt_max (upstroke)
- Resting membrane potential
- APD_min and DI_min
- Adaptation to changes in Cycle length (APD and CV restitution)
- AP Shape at all cycle lengths

Tissue:

- Wave length
- # of singularities
- Dominant frequency
- Life time of singularities

Overview of Project

S Smolka, R Grosu, J. Glimm, R. Gilmour, F. Fenton

Year 3-4

- Quantification of AF initiation and of differences between Normal and disease models.

- Parameter optimization for low voltage FF-AFP

Future Directions

- Apply our expertise in cell modeling to incorporate spatial variability in human ventricular and atrial electrophysiology.

Future Directions

- Use our knowledge and experience in reconstructing three-dimensional tissue structure to develop anatomical models of the human ventricles and atria.

mouse

canine

Canine heart (MRI @120 microns resolution)

Canine heart (DTMRI @ 250 microns resolution)

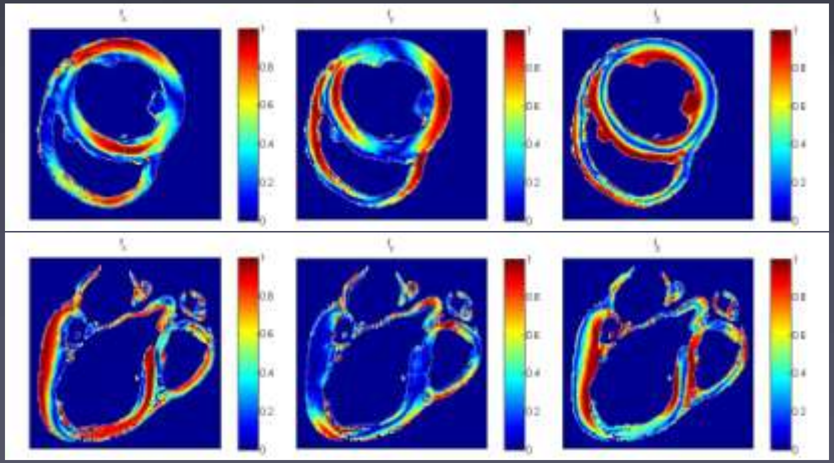

Future Directions

- Use our knowledge and experience in reconstructing three-dimensional tissue structure to develop anatomical models of the human ventricles and atria.

mouse

canine

Canine heart (MRI @120 microns resolution)

Canine heart (DTMRI @ 250 microns resolution)

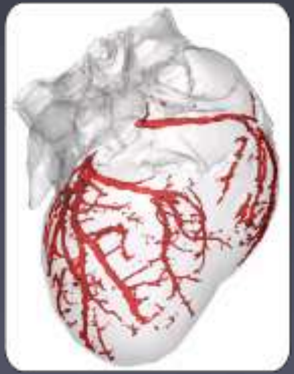

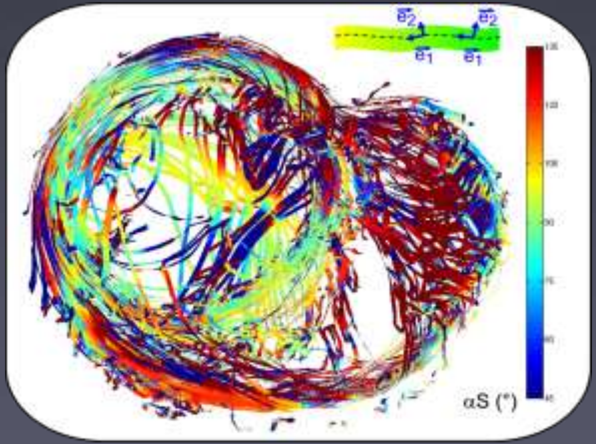

Future Directions

- Use our knowledge and experience in reconstructing three-dimensional tissue structure to develop anatomical models of the human

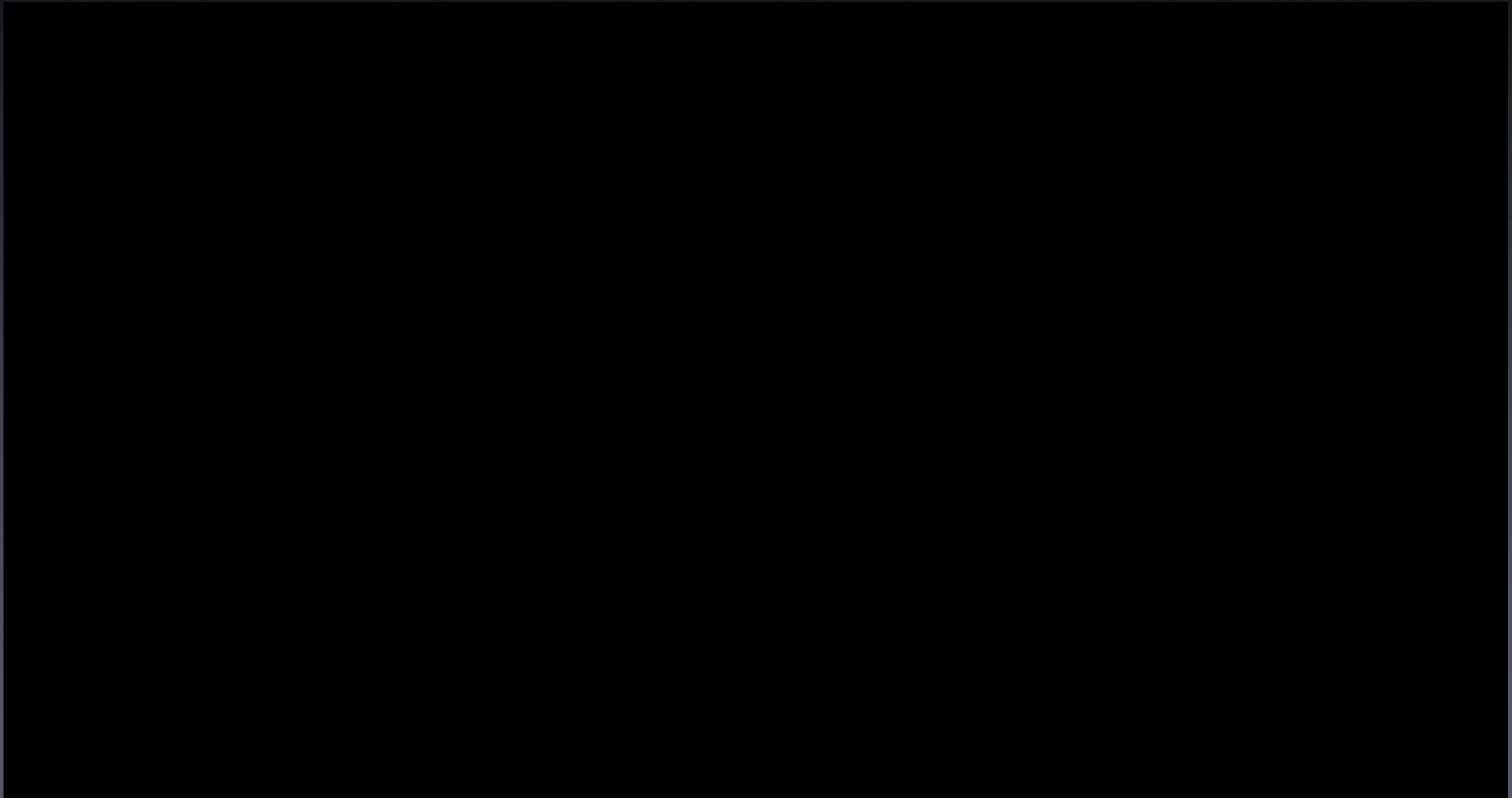

Future Directions

- Apply optical mapping techniques to quantify the properties of arrhythmias in human hearts.

Future Directions

- Apply optical mapping techniques to quantify the properties of arrhythmias in human hearts.

Collaborators

Robert F. Gilmour, Jr.
Eberhard Bodenschatz
Ulrich Parlitz
Stephan Lehnart

http://TheVirtualHeart.org

Support: NSF #0824399 (EMC) and #0800793 (FHF and EMC)
NIH HL075515-S03,-S04 (FHF)
EU FP7 (FHF and SL)